activation-induced proinflammatory cytokine expression by human monocytes and T cells. *J Clin Invest.* 2004; **114**: 57–66.
84. Gonzalez-Rey E, Chorny A, Delgado M. Therapeutic action of ghrelin in a mouse model of colitis. *Gastroenterology.* 2006; **130**: 1707–20.
85. Granado M, Priego T, Martin AI, Villanua A, Lopez-Caldron A. Anti-inflammatory effect of the ghrelin agonist growth hormone-releasing peptide-2 (GHRP-2) in arthritic rats. *Am J Physiol Endocrinol Metab.* 2005; **288**: E486–92.
86. Chorny A, Anderson P, Gonzalez-Rey E, Delgado M. Ghrelin protects against experimental sepsis by inhibiting high-mobility group box 1 release and by killing bacteria. *J Immunol.* 2008; **180**: 8369–77.
87. Wu R, Dong W, Cui X, Zhou M, Simms HH, Ravikumar TS, et al. Ghrelin down-regulates proinflammatory cytokines in sepsis through activation of the vagus nerve. *Ann Surg.* 2007; **245**: 480–6.
88. Theil M-M, Miyake S, Mizuno M, Tomi C, Croxford JL, Hosoda H, et al. Suppression of experimental autoimmune encephalomyelitis by ghrelin. *J Immunol.* 2009; **183**: 2859–66.
89. Miyake S, Yamamura T. Ghrelin: friend or foe for neuroinflammation. *Discov Med.* 2009; **8**: 64–7.
90. Sloan EK, Capitanio JP, Tarara RP, Mendoza SP, Mason WA, Cole SW. Social stress enhances sympathetic innervation of primate lymph nodes: mechanisms and implications for viral pathogenesis. *J Neurosci.* 2007; **27**: 8857–65.
91. Sloan EK, Capitanio JP, Cole SW. Stress-induced remodeling of lymphoid innervation. *Brain Behav Immun.* 2008; **22**: 15–21.
92. Straub RH, Rauch L, Fassold A, Lowin T, Pongratz G. Neuronally released sympathetic neurotransmitters stimulate splenic interferon-gamma secretion from T cells in early type II collagen-induced arthritis. *Arthritis Rheum.* 2008; **58**: 3450–60.
93. Sloan EK, Nguyen CT, Cox BF, Tarara RP, Capitanio JP, Cole SW. SIV infection decreases sympathetic innervation of primate lymph nodes: the role of neurotrophins. *Brain Behav Immun.* 2008; **22**: 185–94.
94. Elenkov IJ, Papanicolaou DA, Wilder RL, Chrousos GP. Modulatory effects of glucocorticoids and catecholamines on human interleukin-12 and interleukin-10 production: clinical implications. *Proc Assoc Am Physicians.* 1996; **108**: 374–81.
95. Le Tulzo Y, Shenkar R, Kaneko D, Moine P, Fantuzzi G, Dinarello CA, et al. Hemorrhage increases cytokine expression in lung mononuclear cells in mice: involvement of catecholamines in nuclear factor-kappaB regulation and cytokine expression. *J Clin Invest.* 1997; **99**: 1516–24.
96. Panina-Bordignon P, Mazzeo D, Lucia PD, D'Ambrosio D, Lang R, Fabbri L, et al. Beta2-agonists prevent Th1 developmenet by selective inhibition of interleukin 12. *J Clin Invest.* 1997; **100**: 1513–9.
97. Kin NW, Sanders VM. It takes nerve to tell T and B cells what to do. *J Leukoc Biol.* 2006; **79**: 1093–104.
98. Strell C, Sievers A, Bastian P, Lang K, Niggemann B, Zänker KS, et al. Divergent effects of norepinephrine, dopamine and substance P on the activation, differentiation and effector functions of human cytotoxic T lymphocytes. *BMC Immunol.* 2009; **8**: 10.
99. Bhowmick S, Singh A, Flavell RA, Clark RB, O'Rourke J, Cone RE. The sympathetic nervous system modulates CD4(+)FoxP3(+) regulatory T cells via a TGF-beta-dependent mechanism. *J Leukoc Biol.* 2009; **86**: 1275–83.
100. Grebe KM, Hickman HD, Irvine KR, Takeda K, Bennink JR, Yewdell JW. Sympathetic nervous system control of anti-influenza CD8+ T cell responses. *Proc Natl Acad Sci USA.* 2009; **106**: 5300–5.
101. Kohm AP, Sanders VM. Norepinephrine and beta 2-adrenergic receptor stimulation regulate CD4+ T and B lymphocyte function in vitro and in vivo. *Pharm Rev.* 2001; **53**: 487–525.
102. Lucin KM, Sanders VM, Jones TB, Malarkey WB, Popovich PG. Impaired antibody synthesis after spinal cord injury is level dependent and is due to sympathetic nervous system dysregulation. *Exp Neurol.* 2007; **207**: 75–84.
103. Harvath L, Robbins JD, Russell AA, Seamon KB. cAMP and human neutrophil chemotaxis. Elevation of cAMP differentially affects chemotactic responsiveness. *J Immunol.* 1991; **146**: 224–32.
104. Barnett CC, Moore EE, Partrick DA, Silliman CC. Beta-adrenergic stimulation down-regulates neutrophil priming for superoxide generation, but not elastase release. *J Surg Res.* 1997; **70**: 166–70.
105. Layé S, Bluthé RM, Kent S, Combe C, Médina C, Parnet P, et al. Subdiaphragmatic vagotomy blocks induction of IL-1 beta mRNA in mice brain in response to peripheral LPS. *Am J Physiol.* 1995; **268**: R1327–31.
106. van Maanen MA, Lebre MC, van der Poll T, LaRosa GJ, Elbaum D, Vervoordeldonk MJ, et al. Stimulation of nicotinic acetylcholine receptors attenuates collagen-induced arthritis in mice. *Arthritis Rheum.* 2009; **60**: 114–22.
107. Borovikova LV, Ivanova S, Zhang M, Yang H, Botchkina GI, Watkins LR, et al. Vagus nerve stimulation attenuates the systemic inflammatory response to endotoxin. *Nature.* 2000; **405**: 458–62.
108. Wang H, Yu M, Ochani M, Amella CA, Tanovic M, Susara S, et al. Nicotinic acetylcholine receptor α7 subunit is an essential regulator of inflammation. *Nature.* 2003; **421**: 384–8.
109. Wang H, Liao H, Ochani M, Justiniani M, Lin X, Yang L, et al. Cholinergic agonists inhibit HMGB1 release and improve survival in experimental sepsis. *Nat Med.* 2004; **10**: 1216–21.

110. Shi FD, Piao WH, Kuo YP, Campagnolo DI, Vollmer TL, Lukas RJ. Nicotinic attenuation of central nervous system inflammation and autoimmunity. *J Immunol.* 2009; **182**: 1730–9.
111. Nizri E, Irony-Tur-Sinai M, Lory O, Orr-Urtreger A, Lavi E, Brenner T. Activation of the cholinergic anti-inflammatory system by nicotine attenuates neuroinflammation via suppression of Th1 and Th17 responses. *J Immunol.* 2009; **183**: 6681–8.
112. Fujii YX, Fujigaya H, Moriwaki Y, Misawa H, Kasahara T, Grando SA, et al. Enhanced serum antigen-specific IgG_1 and proinflammatory cytokine production in nicotinic acetylcholine receptor α7 subunit gene knockout mice. *J Neuroimmunol.* 2007; **189**: 69–74.
113. van der Zanden EP, Snoek SA, Heinsbroek SE, Stanisor OI, Verseijden C, Boeckxstaens GE, et al. Vagus nerve activity augments intestinal macrophage phagocytosis via nicotinic acetylcholine receptor α4β2. *Gastroenterology.* 2009; **189**: 1029–39.
114. Shaked I, Meerson A, Wolf Y, Avni R, Greenberg D, Gilboa-Geffen A, et al. MicroRNA-132 potentiates cholinergic anti-inflammatory signaling by targeting acetylcholinesterase. *Immunity.* 2009; **131**: 965–73.
115. Levite M. Neurotransmitters activate T-cells and elicit crucial functions via neurotransmitter receptors. *Curr Opin Pharmacol.* 2008; **8**: 460–71.
116. Nakano K, Higashi T, Takagi R, Hashimoto K, Tanaka Y, Matsushita S. Dopamine released by dendritic cells polarizes Th2 differentiation. *Int Immunol.* 2009; **21**: 645–54.
117. Bergquist J, Tarkowski A, Ekman R, Ewing A. Discovery of endogenous catecholamines in lymphocytes and evidence for catecholamine regulation of lymphocyte function via an autocrine loop. *Proc Natl Acad Sci USA.* 1994; **91**: 12912–6.
118. Flierl MA, Rittirsch D, Nadeau BA, Chen AJ, Sarma V, Zetoune F, et al. Phagocyte-derived catecholamines enhance acute inflammatory injury. *Nature.* 2007; **449**: 721–6.
119. Cosentino M, Fietta AM, Ferrari M, Rasini E, Bombelli R, Carcano E, et al. Human $CD4^+CD25^+$ regulatory T cells selectively express tyrosine hydroxylase and contain endogenous catecholamines subserving an autocrine/paracrine inhibitory functional loop. *Blood.* 2007; **109**: 632–42.
120. Agulia MC, Dees WL, Haensly WE, McCann M. Evidence that somatostatin is localized and synthesized in lymphoid organs. *Proc Natl Acad Sci USA.* 1991; **88**: 11485–9.
121. De Giorgio R, Tazzari PL, Barbara G, Stanhellini V, Corinaldesi R. Detection of substance P immunoreactivity in human peripheral leukocytes. *J Neuroimmunol.* 1998; **82**: 175–81.
122. Li Y, Tian S, Douglas SD, Ho WZ. Morphine up-regulates expression of substance P and its receptor in human blood mononuclear phagocytes and lymphocytes. *Cell Immunol.* 2000; **205**: 120–7.
123. Qian BF, Zhou GQ, Hammarstrom ML, Danielsson A. Both substance P and its receptor are expressed in mouse intestinal T lymphocytes. *Neuroendocrinology.* 2001; **73**: 358–68.
124. Arsenescu R, Blum AM, Metwali A, Elliott DE, Weinstock JV. IL-12 induction of mRNA encoding substance P in murine macrophages from the spleen and sites of inflammation. *J Immunol.* 2005; **174**: 3906–11.
125. Mousa SAStraub R, Schafer M, Stein C. Beta-endorphin, Met-enkephalin and corresponding opioid receptors within synovium of patients with joint trauma, osteoarthritis and rheumatoid arthritis. *Ann Rheum Dis.* 2007; **66**: 871–9.
126. Bracci-Laudiero L, Aloe L, Buanne P, Finn A, Stenfors C, Vigneti E, et al. NGF modulates CGRP synthesis in human B-lympho cytes: a possible anti-inflammatroy action on NGF? *J Neuroimmunol.* 2002; **123**: 58–65.
127. Bracci-Laudiero L, Aloe L, Caroleo MC, Buanne P, Costa NStarace G, et al. Endogenous NGF regulates CGRP expression in human monocytes, and affects HLA-DR and CD86 expression and IL-10 production. *Blood.* 2005; **106**: 3507–14.
128. Xing L, Guo J, Wang X. Induction and expression of β-calcitonin gene-related peptide in rat T lymphocytes and its significance. *J Immunol.* 2000; **165**: 4359–66.
129. Gomariz RP, Leceta J, Garrido E, Garrido T, Delgado M. Vasoactive intestinal peptide (VIP) mRNA expression in rat T and B lymphocytes. *Regul Pept.* 1994; **50**: 177–84.
130. Martinez C, Delgado M, Abad C, Gomariz RP, Ganea D, Leceta J. Regulation of VIP production and secretion by murine lymphocytes. *J Neuroimmunol.* 1999; **93**: 126–38.
131. Ganor Y, Besser M, Ben-Zakay N, Unger T, Levite M. Human T cells express a functional ionotropic glutamate receptor GluR3, and glutamate by itself triggers integrin-mediated adhesion to laminin and fibronectin and chemotactic migration. *J Immunol.* 2003; **170**: 4362–72.
132. Pitt D, Werner P, Paine CS. Glutamate excitotoxicity in a model of multiple sclerosis. *Nat Med.* 2000; **6**: 67–70.
133. Pacheco R, Oliva H, Martinez-Navio JM, Climent N, Ciruela F, Gatell JM, et al. Glutamate released by dendritic cells as a novel modulator of T cell activation. *J Immunol.* 2006; **177**: 6695–704.
134. Pacheco R, Ciruela F, Casado V, Mallol J, Gallart T, Lluis C, et al. Group I metabotropic glutamate receptors mediate a dual role of glutamate in T cell activation. *J Biol Chem.* 2004; **279**: 33352–8.
135. Fallarino F, Volpi C, Fazio F, Notartomaso S, Vacca C, Busceti C, et al. Metabotropic glutamate receptor-4 modulates adaptive immunity and restrains neuroinflammation. *Nat Med.* 2010; **16**: 897–902.
136. Bergquist J, Josefsson E, Tarkowski A, Ekman R, Ewing A. Measurements of catecholamine-mediated apoptosis of immunocompetent cells by capillary electrophoresis. *Electrophoresis.* 1997; **18**: 1760–6.

137. Ghosh MC, Mondal AC, Basu S, Banerjee S, Majumdar J, Bhattacharya D, et al. Dopamine inhibits cytokine release and expression of tyrosine kinases, Lck and Fyn in activated T cells. *Int Immunopharmacol.* 2003; **3**: 1019–26.
138. Missale C, Nash SR, Robinson SW, Jaber M, Caron MG. Dopamine receptors: from structure to function. *Physiol Rev.* 1998; **78**: 189–225.
139. Saha B, Mondal AC, Majumder J, Basu S, Dasgupta PS. Physiological concentrations of dopamine inhibit the proliferation and cytotoxicity of human CD4+ and CD8+ T cells in vitro: a receptor-mediated mechanism. *Neuroimmunomodulation.* 2001; **9**: 23–33.
140. Kipnis J, Cardon M, Avidan H, Lewitus GM, Mordechay S, Rolls A, et al. Dopamine, through the extracellular signal regulated kinase pathway, downregulates CD4+CD25+ regulatory T-cell activity: implications for neurodegeneration. *J Neurosci.* 2004; **4**: 6133–43.
141. Levite M, Chowers Y, Ganor Y, Besser M, Hershkovits R, Cahalon L. Dopamine interacts directly with its D3 and D2 receptors on normal human T cells, and activates beta1 integrin function. *Eur J Immunol.* 2001; **31**: 3504–12.
142. Besser MJ, Ganor Y, Levite M. Dopamine by itself activates either D2, D3 or D1/D5 dopaminergic receptors in normal human T-cells and triggers the selective secretion of either IL-10, TNFalpha or both. *J Neuroimmunol.* 2005; **169**: 161–71.
143. Watanabe Y, Nakayama T, Nagakubo D, Hieshima K, Jin Z, Katou F, et al. Dopamine selectively induces migration and homing of naive CD8+ T cells via dopamine receptor D3. *J Immunol.* 2006; **176**: 848–56.
144. Nakano K, Higashi T, Hashimoto K, Takagi Ri, Tanaka Y, Matsushita S. Antagonizing dopamine D1-like receptor inhibits Th17 cell differentiation: preventive and therapeutic effects on experimental autoimmune encephalomyelitis. *Biochem Biophys Res Commun.* 2008; **373**: 286–91.
145. Nakano K, Yamaoka K, Hanami K, Saito K, Sasaguri Y, Yanagihara N, et al. Dopamine induces IL-6-dependent IL-17 production via D1-like receptor on CD4 Naïve T cells and D1-like receptor antagonist SCH-23390 inhibits cartilage destruction in a human rheumatoid arthritis/SCID mouse chimera model. *J Immunol.* 2011; **186**: 3745–52.
146. Lotz M, Vaughan JH, Carson DA. Effects of neuropeptides on production of inflammatory cytokines by human monocytes. *Science.* 1988; **241**: 1218–21.
147. Calvo CF, Chavanel G, Senik A. Substance P enhances IL-2 expression in activated human T cells. *J Immunol.* 1992; **148**: 3498–504.
148. Mathers AR, Tckacheva OA, Janelsins BM, Shufesky WJ, Morelli AE, Larregina AT. In vivo signaling through the neurokinin 1 receptor favors transgene expression by Langerhans cells and promotes the generation of Th1- and Tc1-biased immune responses. *J Immunol.* 2007; **178**: 7006–17.
149. Cunin P, Caillon A, Corvaisier M, Garo E, Scotet M, Blanchard S, et al. The tachykinins substance P and hemokinin-1 favor the generation of human memory Th17 cells by inducing IL-1β, Il-23, and TNF-like 1A expression by monocytes. *J Immunol.* 2011; **186**: 4175–82.
150. Hegde A, Zhang H, Moochhala SM, Bhatia M. Neurokinin-1 receptor antagonist treatment protects mice against lung injury in polymicrobial sepsis. *J Leukoc Biol.* 2007; **82**: 678–85.
151. Gad M, Pedersen AE, Kristensen NN, Fernandez Cde F, Claesson MH. Blockage of the neurokinin 1 receptor and capsaicin-induced ablation of the enteric afferent nerves protect SCID mice against T-cell-induced chronic colitis. *Inflamm Bowel Dis.* 2009; **15**: 1174–82.
152. Hegde A, Koh YH, Moochhala SM, Bhatia M. Neurokinin-1 receptor antagonist treatment in polymicrobial sepsis: molecular insights. *Int J Inflam.* 2010; **2010**: 601098.
153. Dantzer R, O'Connor JC, Freund GG, Johnson RW, Kelley KW. From inflammation to sickness and depression: when the immune system subjugates the brain. *Nat Rev Neurosci.* 2008; **9**: 46–57.
154. Rettori V, Gimeno MF, Karara A, Gonzalez MC, McCann SM. Interleukin 1 alpha inhibits prostaglandin E2 release to suppress pulsatile release of luteinizing hormone but not follicle-stimulating hormone. *Proc Natl Acad Sci USA.* 1991; **88**: 2763–7.
155. Bluthé RM, Kelley KW, Dantzer R. Effects of insulin-like growth factor-I on cytokine-induced sickness behavior in mice. *Brain Behav Immun.* 2006; **20**: 57–63.
156. Dantzer R, Gheusi G, Johnson RW, Kelley KW. Central administration of insulin-like growth factor-1 inhibits lipopolysaccharide-induced sickness behavior in mice. *Neuroreport.* 1999; **10**: 289–92.
157. Dantzer R, Gheusi G, Johnson RW, Kelley KW. Central injection of IL-10 antagonizes the behavioural effects of lipopolysaccharide in rats. *Psychoneuroendocrinology.* 1999; **24**: 301–11.
158. Leon LR, Kozak W, Rudolph K, Kluger MJ. An antipyretic role for interleukin-10 in LPS fever in mice. *Am J Physiol.* 1999; **276**: R81–9.
159. Perkins MN, Stone TW. An iontophoretic investigation of actions of convulsant kynurenines and their interaction with endogenous excitant quinolinic acid. *Brain Res.* 1982; **247**: 184–7.
160. Kerschensteiner M, Gallmeier E, Behrens L, Leal VV, Misgeld T, Klinkert WE, et al. Activated human T cells, B cells, and monocytes produce brain-derived neurotrophic factor in vitro and in inflammatory brain lesions: a neuroprotective role of inflammation? *J Exp Med.* 1999; **189**: 865–70.
161. Kipnis J, Cohen H, Cardon M, Ziv Y, Schwartz M. T cell deficieny leads to cognitive dysfunction: implications

for therapeutic vaccination for schizophrenia and other psychiatric conditions. *Proc Natl Acad Sci USA*. 2004; **101**: 8180–5.
162. Ziv Y, Ron N, Butovsky O, Landa G, Sudai E, Greenberg N, et al. Immune cells contribute to the maintenance of neurogenesis and spatial learning abilities in adulthood. *Nat Neurosci*. 2006; **9**: 268–75.
163. Wolf SA, Steiner B, Akpinarli A, Kammertoens T, Nassenstein C, Braun A, et al. CD4-positive T lymphocytes provide a neuroimmunological link in the control of adult hippocampal neurogenesis. *J Immunol*. 2009; **182**: 3979–84.
164. Abbas N, Bednar I, Mix E, Marie S, Paterson DL, Jungberg A, et al. Up-regulation of the inflammatory cytokines IFN-gamma and IL-12 and down-regulation of IL-4 in cerebral cortex regions of APP(SWE) transgenic mice. *J Neuroimmunol*. 2002; **126**: 50–7.
165. Straub RH, Dhabhar FS, Bijlsma WJ, Cutolo M. How psychological stress via hormones and nerve fibers may exacerbate rheumatoid arthritis. *Arthritis Rheum*. 2005; **52**: 16–26.
166. Jara LJ, Navarro C, Medina G, Vera-Lastra O, Blanco F. Immune-neuroendocrine interactions and autoimmune diseases. *Clin Dev Immunol*. 2006; **13**: 109–23.

ARTHRITIS & RHEUMATISM
Vol. 64, No. 1, January 2012, pp 153–161
DOI 10.1002/art.33314

Mucosal-Associated Invariant T Cells Promote Inflammation and Exacerbate Disease in Murine Models of Arthritis

Asako Chiba, Ryohsuke Tajima, Chiharu Tomi, Yusei Miyazaki, Takashi Yamamura, and Sachiko Miyake

Objective. **The function of mucosal-associated invariant T (MAIT) cells remains largely unknown. We previously reported an immunoregulatory role of MAIT cells in an animal model of multiple sclerosis. The aim of this study was to use animal models to determine whether MAIT cells are involved in the pathogenesis of arthritis.**

Methods. **$MR1^{-/-}$ and $MR1^{+/+}$ DBA/1J mice were immunized with bovine type II collagen (CII) in complete Freund's adjuvant to trigger collagen-induced arthritis (CIA). To assess CII-specific T cell recall responses, lymph node cells from mice with CIA were challenged with CII ex vivo, and cytokine production and proliferation were evaluated. Serum levels of CII-specific antibodies were measured by enzyme-linked immunosorbent assay. Collagen antibody–induced arthritis (CAIA) was induced in $MR1^{-/-}$ and $MR1^{+/+}$ C57BL/6 mice by injection of anti-CII antibodies followed by injection of lipopolysaccharide. To demonstrate the involvement of MAIT cells in arthritis, we induced CAIA in $MR1^{-/-}$ C57BL/6 mice that had been reconstituted with adoptively transferred MAIT cells. MAIT cell activation in response to cytokine stimulation was investigated.**

Results. **The severity of CIA was reduced in $MR1^{-/-}$ DBA/1J mice. However, T and B cell responses to CII were comparable in $MR1^{-/-}$ and $MR1^{+/+}$ DBA/1J mice. $MR1^{-/-}$ C57BL/6 mice were less susceptible to CAIA, and reconstitution with MAIT cells induced severe arthritis in $MR1^{-/-}$ C57BL/6 mice, demonstrating an effector role of MAIT cells in arthritis. MAIT cells became activated upon stimulation with interleukin-23 (IL-23) or IL-1β in the absence of T cell receptor stimuli.**

Conclusion. **These results indicate that MAIT cells exacerbate arthritis by enhancing the inflammation.**

Rheumatoid arthritis (RA) is an autoimmune disease characterized by chronic inflammation in the joints. It has been suggested that environmental factors influence autoimmunity, and in particular, increasing evidence highlights the important role of gut flora in the development of autoimmune diseases (1), including arthritis. For example, differences in the intestinal microbiota of patients with early RA have been described, and tetracycline treatment was shown to reduce disease activity in RA (2,3). In addition, oral vancomycin treatment significantly decreased the severity of adjuvant-induced arthritis (4). More recently, it was demonstrated that germ-free conditions strongly inhibit arthritis in the K/BxN arthritis model and that the introduction of segmented filamentous bacteria induced severe arthritis in germ-free K/BxN mice (5). Thus, mucosal immunity plays an important role in the development and progression of arthritis.

Natural killer (NK) cells, invariant NK T (iNKT) cells, γ/δ T cells, mucosal-associated invariant T (MAIT) cells, B-1 B cells, and marginal-zone B cells are categorized as innate-like lymphocytes. Such lymphocytes reside in unique locations, including the marginal zone of the spleen and epithelial and mucosal tissues and rapidly exert effector functions in the absence of clonal expansion (6–15). Therefore, these innate-like lymphocytes are thought to play important roles in "first-line" im-

Supported by the Japan Foundation for Neuroscience and Mental Health (to Dr. Chiba), the Japan Rheumatism Foundation (to Dr. Chiba), the Japan Society for the Promotion of Science (Grants-in-Aid for Scientific Research B: 20390284 and 23390261 to Dr. Miyake), and the Ministry of Health, Labor, and Welfare of Japan (Health and Labor Sciences Research Grants on Intractable Diseases).

Asako Chiba, MD, PhD, Ryohsuke Tajima, MS, Chiharu Tomi, Yusei Miyazaki MD, PhD, Takashi Yamamura MD, PhD, Sachiko Miyake MD, PhD: National Institute of Neuroscience, National Centre of Neurology and Psychiatry, Tokyo, Japan.

Address correspondence to Sachiko Miyake MD, PhD, Department of Immunology, National Institute of Neuroscience, National Centre of Neurology and Psychiatry, 4-1-1 Ogawahigashi, Kodaira, Tokyo 187-8502, Japan. E-mail: miyake@ncnp.go.jp.

Submitted for publication May 15, 2011; accepted in revised form August 25, 2011.

mune responses against exogenous stimuli. As MAIT cells are preferentially located in the gut lamina propria, there is a growing interest in the function of MAIT cells in various types of immune responses, including autoimmunity (16–20).

MAIT cells are restricted by a nonpolymorphic class IB major histocompatibility complex (MHC) molecule, the class I MHC–related molecule (MR1), and express an invariant T cell receptor (TCR) α-chain: V_α7.2–J_α33 in humans and V_α19–J_α33 in mice. The invariant TCRα chain associates with a limited set of V_β chains (14,21,22). MAIT cells are selected in the thymus in an MR1-dependent manner, but, interestingly, MAIT cells require B cells as well as commensal flora for their peripheral expansion (14,23). Our group previously demonstrated a protective role of MAIT cells against autoimmune encephalomyelitis (EAE), an animal model of human multiple sclerosis. The suppression of EAE was accompanied by increased production of interleukin-10 (IL-10) by B cells, which was induced in part by ICOS costimulation (17). Because the invariant V_α7.2–J_α33 TCR is highly expressed in central nervous system lesions of multiple sclerosis patients, human MAIT cells may also be involved in the pathogenesis of multiple sclerosis (16).

In addition to their regulatory function, MAIT cells also possess proinflammatory functions like other innate-like lymphocytes. Le Bourhis et al (20) demonstrated that MAIT cells display antimicrobial capacity. Both human and mouse MAIT cells are activated by *Escherichia coli*–infected antigen-presenting cells in an MR1-dependent manner. MAIT cells show a protective role against *Mycobacterium abscessus* or *E coli* infections in mice. Human MAIT cells are capable of producing interferon-γ (IFNγ) and IL-17 and are found in *Mycobacterium tuberculosis*–infected lung tissues. Thus, MAIT cells play an antimicrobial function under these infectious conditions. Although accumulating evidence suggests that certain subsets of innate-like lymphocytes, such as NK cells, iNKT cells, and γ/δ T cells, are involved in the pathogenesis of arthritis in animal models of the disease, the role of MAIT cells in arthritis remains unknown (24–31).

We report herein that MAIT cells play a pathogenic role in murine models of arthritis. The disease severity of collagen-induced arthritis (CIA) in MAIT cell–deficient $MR1^{-/-}$ DBA/1J mice was ameliorated compared with that of $MR1^{+/+}$ DBA/1J mice. However, T cell responses to type II collagen (CII) and CII-specific serum antibody levels were comparable between CIA-induced $MR1^{-/-}$ and $MR1^{+/+}$ DBA/1J mice. We found that $MR1^{-/-}$ C57BL/6J mice are much less susceptible to collagen antibody–induced arthritis (CAIA) as compared to $MR1^{+/+}$ C57BL/6J mice. $MR1^{-/-}$ C57BL/6J mice reconstituted with adoptively transferred MAIT cells developed severe arthritis, suggesting that MAIT cells may be one of the effectors contributing to inflammation in arthritis. Finally, we investigated the cytokine-producing capacity of MAIT cells. No differences in IFNγ production by liver mononuclear cells (LMNCs) from $MR1^{-/-}$ C57BL/6J and $MR1^{+/+}$ C57BL/6J mice were observed upon TCR stimulation, but the level of IL-17 produced by LMNCs from $MR1^{+/+}$ C57BL/6J mice was much higher than that produced by cells from $MR1^{-/-}$ C57BL/6J mice. We further demonstrated that sorted murine MAIT cells produce IL-17 upon TCR engagement. Surprisingly, IL-17 production by MAIT cells was observed after exposure to IL-23 without TCR stimulation, and IL-1β alone induced proliferation of MAIT cells, indicating that MAIT cells may be activated by cytokines and may enhance the inflammation in arthritis.

MATERIALS AND METHODS

Mice. DBA/1J mice were purchased from the Oriental Yeast Company. C57BL/6J mice were obtained from CLEA Laboratory Animal Corporation. $MR1^{-/-}$ mice (14) were provided by S. Gilfillan (Department of Pathology and Immunology, Washington University School of Medicine, St. Louis, MO), and V_α19i-transgenic mice (32) on a C57BL/6J background were provided by M. Shimamura (University of Tsukuba, Ibaraki, Japan). $MR1^{-/-}$ mice were backcrossed to DBA/1J mice for 10 generations to obtain $MR1^{-/-}$ DBA/1J mice. V_α19i-transgenic $CD1d1^{-/-}$ C57BL/6J mice were generated by backcrossing V_α19i-transgenic mice with $CD1d1^{-/-}$ C57BL/6J mice for 7 generations. Mice were maintained under specific pathogen–free conditions in accordance with institutional guidelines and used in the experiments at 7–12 weeks of age.

Induction of CIA. Both $MR1^{-/-}$ DBA/1J mice and their littermate controls ($MR1^{+/+}$ DBA/1J mice) (n = 5–6 per group; ages 7–8 weeks old) were immunized intradermally at the base of the tail with 150 μg of CII (Collagen Research Center) emulsified with an equal volume of complete Freund's adjuvant containing 250 μg of heat-killed *Mycobacterium tuberculosis* H37Ra (Difco). Three weeks after the primary immunization, mice were given an intradermal booster injection of 150 μg of CII emulsified in incomplete Freund's adjuvant (Difco).

Induction of CAIA. $MR1^{-/-}$ C57BL/6J mice and their littermate controls ($MR1^{+/+}$ C57BL/6J mice) were injected intravenously with a mixture of anti-CII monoclonal antibodies (mAb) (Arthrogen-CIA mAb, 2 mg; Chondrex) followed 2 days later by an intraperitoneal injection of 50 μg of lipopolysaccharide.

Clinical assessment of arthritis. Mice were examined for signs of joint inflammation, which was scored on a scale of 0–4, where 0 = no change, 1 = significant swelling and redness

of 1 digit, 2 = mild swelling and erythema of the limb or swelling of ≥2 digits, 3 = marked swelling and erythema of the limb, and 4 = maximal swelling and redness of the limb and later, ankylosis. The average macroscopic score was expressed as a cumulative value for all paws, with a maximum possible score of 16.

Histopathologic assessment. Arthritic mice were killed, and all 4 paws were fixed in buffered formalin, decalcified, embedded in paraffin, sectioned, and then stained with hematoxylin and eosin. Histologic assessment of joint inflammation was scored on a scale of 0–3 as follows: 0 = normal joint, 1 = mild arthritis (minimal synovitis without cartilage/bone erosion), 2 = moderate arthritis (synovitis and erosion but joint architecture maintained), and 3 = severe arthritis (synovitis, erosion, and loss of joint integrity). The average of the macroscopic scores was expressed as a cumulative value for all paws, with a maximum possible score of 12.

CII-specific T cell response. Lymph node cells were collected on days 35–42 after immunization and suspended in complete RPMI 1640 medium (Life Technologies) containing 1% syngeneic mouse serum. The cells were cultured for 72 hours in 96-well flat-bottomed plates at a density of 1×10^6/well in the presence of CII. Proliferative responses were measured using a β-1205 counter (Pharmacia) to detect the incorporation of ^{3}H-thymidine (1 μCi/well) during the final 16 hours of culture.

Measurement of CII-specific total IgG, IgG1, and IgG2a. Bovine CII (1 mg/ml) was coated onto enzyme-linked immunosorbent assay (ELISA) plates (Sumitomo Bakelite) overnight at 4°C. After blocking with 1% bovine serum albumin in PBS, serially diluted serum samples were added to CII-coated wells. For detection of anti-CII antibodies, the plates were incubated with biotin-labeled anti-IgG1 and anti-IgG2a (SouthernBiotech) or anti-IgG antibody (CN/Cappel) for 1 hour and were then incubated with streptavidin–peroxidase. After adding substrate, the reaction was evaluated as the optical density values at 450 nm (OD_{450}).

Adoptive transfer and in vitro stimulation of V_α19i T cells. LMNCs were purified from V_α19i-transgenic CD1d1$^{-/-}$ C57BL/6J mice by use of Percoll density-gradient centrifugation, and erythrocytes and B cells were depleted with phycoerythrin (PE)–conjugated anti–Ter-119 and PE-conjugated anti-CD19 (BD) followed by separation with anti–PE-conjugated magnetic-activated cell sorter beads (Miltenyi Biotec). Cells were stained with fluorescein isothiocyanate–conjugated anti-TCRβ and PerCP–Cy5.5 anti-NK1.1 (BD), and TCRβ+ NK1.1+ cells were sorted using a FACSAria cell sorter (BD). The purity of isolated NK1.1+ T cells (MAIT cells) was >95%, as assessed by flow cytometry.

In adoptive transfer experiments, 5×10^5 MAIT cells or NK1.1– T cells (T cells) were injected intravenously into naive MR1$^{-/-}$ C57BL/6 recipient mice 1 day before administration of CII mAb. LMNCs or sorted MAIT cells were resuspended in RPMI 1640 medium supplemented with 10% fetal bovine serum, 2 m*M* L-glutamine, 50 units/ml of penicillin/streptomycin, and 55 μ*M* β-mercaptoethanol (Life Technologies) and stimulated with immobilized anti-CD3 mAb (2C11, 1 μg/ml) and/or the following cytokines: IL-1β, tumor necrosis factor α (TNFα), IL-6, and transforming growth factor β (TGFβ) (all from PeproTech) and IL-23 (R&D Systems).

Detection of cytokines. Cytokine levels in the culture supernatant were determined using a sandwich ELISA. The ELISA antibodies for IFNγ were purchased from BD. Levels of IL-17 were determined using an IL-17 ELISA kit (R&D Systems).

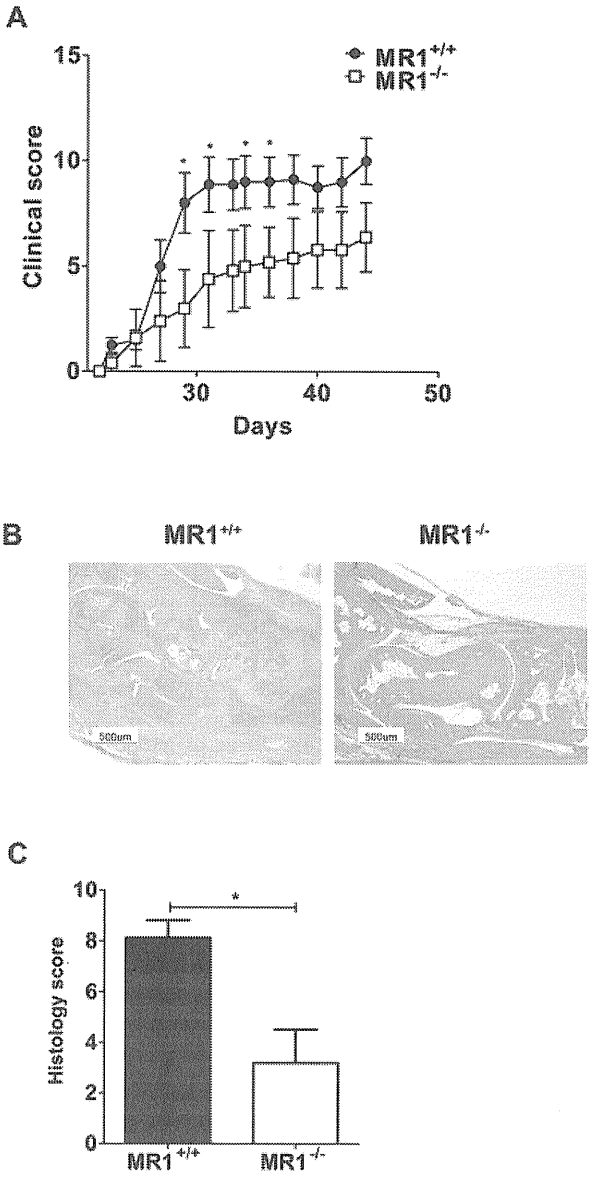

Figure 1. Amelioration of collagen-induced arthritis (CIA) in MR1$^{-/-}$ mice. A, Clinical scores for CIA in MR1$^{-/-}$ DBA/1J mice and in MR1$^{+/+}$ DBA/1J mice. Values are the mean ± SEM of 5–8 mice per group. * = $P < 0.05$ versus MR1$^{-/-}$ DBA/1J mice. B, Representative histologic sections of the joints of MR1$^{+/+}$ DBA/1J mice and MR1$^{-/-}$ DBA/1J mice. Hematoxylin and eosin stained; original magnification × 40. C, Histology scores in MR1$^{-/-}$ DBA/1J mice and in MR1$^{+/+}$ DBA/1J mice, expressed as the sum of the scores in the 4 paws. Results from a single representative experiment of 2 similar experiments performed are shown. Values are the mean ± SEM. * = $P < 0.05$.

Statistical analysis. Clinical or pathologic scores for CIA and CAIA in the various groups of mice are presented as

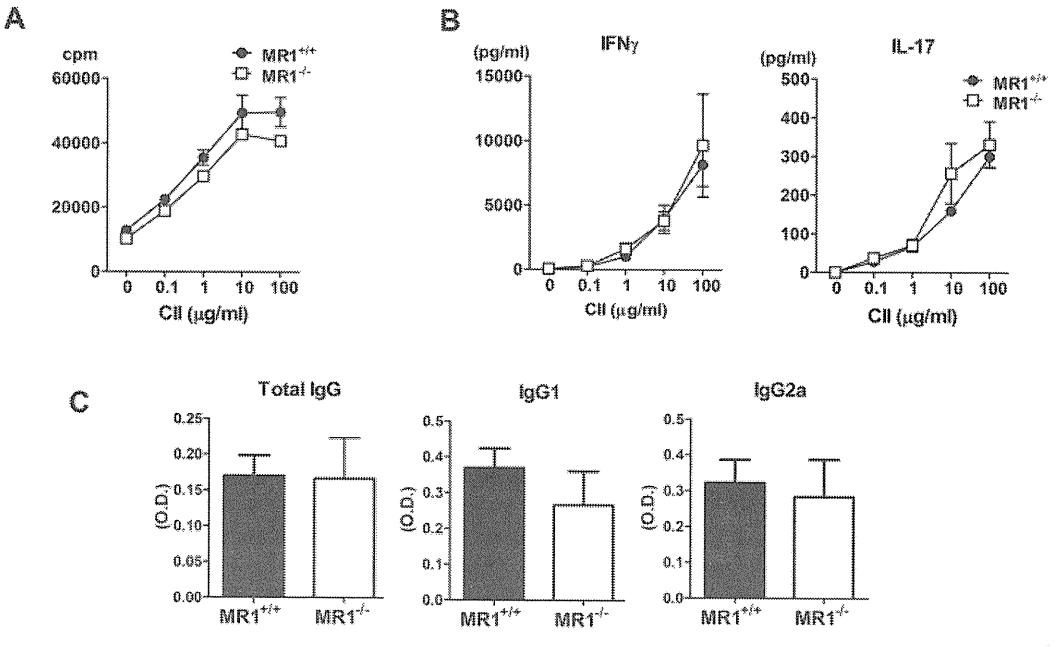

Figure 2. Type II collagen (CII) responses in MR1$^{-/-}$ DBA/1J mice. A and B, Inguinal lymph node cells from MR1$^{-/-}$ DBA/1J mice and MR1$^{+/+}$ DBA/1J mice with collagen-induced arthritis were incubated for 48 hours in the presence of CII. Proliferative responses were determined by the uptake of ^{3}H-thymidine (A), and the levels of interferon-γ (IFNγ) and interleukin-17 (IL-17) in culture supernatants were measured by enzyme-linked immunosorbent assay (B). C, CII-specific antibody levels in individual serum samples obtained at the end of the experiment were analyzed as described in Materials and Methods. Results from a single representative experiment of 2 similar experiments performed are shown. Values are the mean ± SEM of 5–8 mice per group. OD = optical density

the mean ± SEM clinical score for the group, and statistical differences were analyzed with a nonparametric Mann-Whitney U test. Data for cytokines and proliferation were analyzed with an unpaired *t*-test.

RESULTS

Amelioration of CIA in MR1$^{-/-}$ mice. To investigate whether MAIT cells play a role in the pathogenesis of arthritis, we first evaluated the involvement of MAIT cells in CIA using MR1$^{-/-}$ mice lacking MAIT cells. Because DBA/1J mice bearing the H-2q haplotype are the most susceptible strain for CIA, MR1$^{-/-}$ C57BL/6J mice were backcrossed to DBA/1J mice for 10 generations to obtain MR1$^{-/-}$ DBA/1J mice. Both MR1$^{-/-}$ DBA/1J mice and littermate MR1$^{+/+}$ DBA/1J mice were immunized with CII to induce CIA, and the clinical severity of arthritis was evaluated by visual scoring of each paw. As shown in Figure 1A, the clinical scores in MR1$^{-/-}$ DBA/1J mice were reduced in comparison to those in MR1$^{+/+}$ DBA/1J mice. Histologic examination of the joints of the 4 paws 44 days after CIA induction showed less cell infiltration, cartilage erosion, and bone destruction in MR1$^{-/-}$ DBA/1J mice than in the MR1$^{+/+}$ DBA/1J mice (Figure 1B). Quantification of the histologic severity of arthritis revealed that MR1$^{-/-}$ DBA/1J mice developed milder joint inflammation than MR1$^{+/+}$ DBA/1J mice (Figure 1C). These results suggest that MAIT cells contribute to the exacerbation of the disease course of CIA.

CII responses in MR1$^{-/-}$ DBA/1J mice. As the presence of MAIT cells augmented the severity of CIA, we next asked whether MAIT cells influence the CII-specific responses of T and B cells. Lymph node cells from CIA-induced animals were rechallenged with CII ex vivo. As shown in Figure 2A, the proliferative responses of lymph node cells upon stimulation with CII were similar in the two groups. Lymph node cells from both MR1$^{-/-}$ DBA/1J mice and MR1$^{+/+}$ DBA/1J mice produced comparable amounts of IL-17 and IFNγ in response to CII in a dose-dependent manner (Figure 2B). We also evaluated CII-specific immunoglobulin levels in serum obtained 35-42 days after arthritis induction. We observed a trend of reduced levels of CII-specific IgG1 in MR1$^{-/-}$ DBA/1J mice compared to the

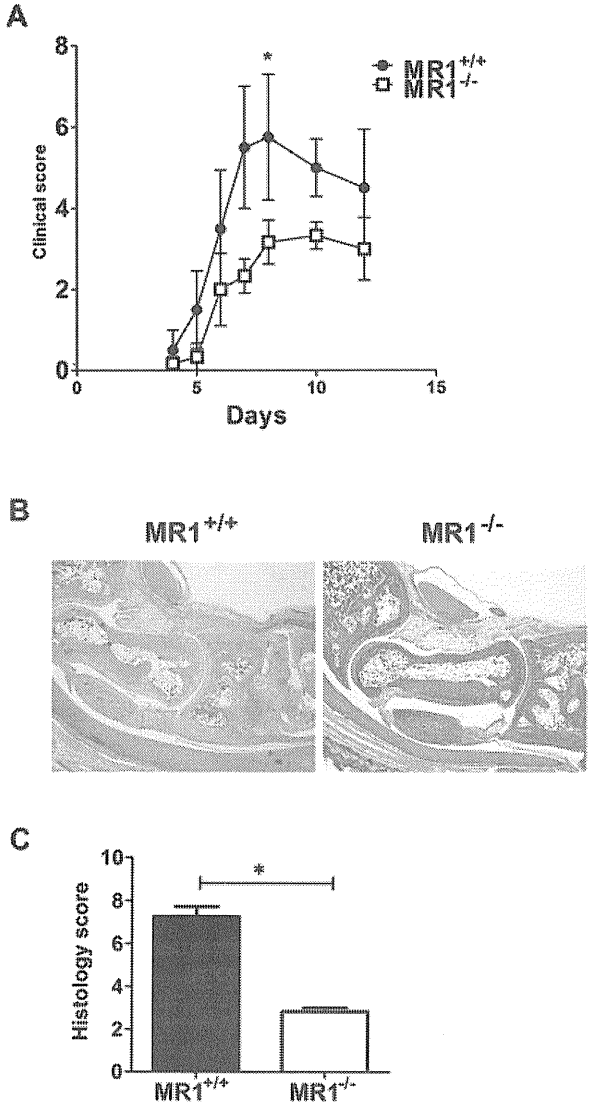

Figure 3. Amelioration of collagen antibody–induced arthritis (CAIA) in $MR1^{-/-}$ mice. A, Clinical scores for CAIA in $MR1^{-/-}$ C57BL/6J mice and $MR1^{+/+}$ C57BL/6J mice. Values are the mean ± SEM of 4–6 mice per group. * = $P < 0.05$ versus $MR1^{-/-}$ C57BL/6J mice. B, Representative histologic sections of the joints of $MR1^{+/+}$ C57BL/6J mice and $MR1^{-/-}$ C57BL/6J mice. Hematoxylin and eosin stained; original magnification × 40. C, Histology scores in $MR1^{-/-}$ C57BL/6J mice and in $MR1^{+/+}$ C57BL/6J mice, expressed as the sum of the scores in the 4 paws. Results from a single representative experiment of 2 similar experiments performed are shown. Values are the mean ± SEM. * = $P < 0.05$.

levels in $MR1^{+/+}$ DBA/1J mice, but the difference did not reach statistical significance (Figure 2C). These results indicate that the presence of MAIT cells has little effect on CII-specific responses.

Amelioration of CAIA in $MR1^{-/-}$ mice. The CIA model requires both adaptive and innate immune responses for disease development, and T cells and B cells responding to CII are the major players in the initiation of the disease. Although we observed significant differences in both the clinical and pathologic severity of arthritis when comparing $MR1^{-/-}$ DBA/1J mice to $MR1^{+/+}$ DBA/1J mice (Figure 1), the CII-specific responses of T and B cells appeared not to depend on the presence of MAIT cells (Figure 2). Thus, we hypothesized that MAIT cells may influence the effector phase of arthritis. To test this hypothesis, we induced CAIA in $MR1^{-/-}$ and $MR1^{+/+}$ C57BL/6J mice. By 7 days after injection of anti-CII mAb, $MR1^{+/+}$ C57BL/6J mice had developed severe arthritis, as assessed by clinical scores (Figure 3A). In contrast, the clinical scores in the $MR1^{-/-}$ C57BL/6J mice were lower compared to those in the $MR1^{+/+}$ C57BL/6J mice. Histologic assessment 10 days after arthritis induction revealed severe arthritis with leukocyte infiltration, synovial hyperplasia, pannus formation, cartilage erosion, and bone destruction in $MR1^{+/+}$ C57BL/6J mice, whereas these features were milder in $MR1^{-/-}$ C57BL/6J mice (Figures 3B and C).

Augmentation of arthritis in $MR1^{-/-}$ mice by adoptive transfer of MAIT cells. To demonstrate that MAIT cells actually enhance disease severity in the

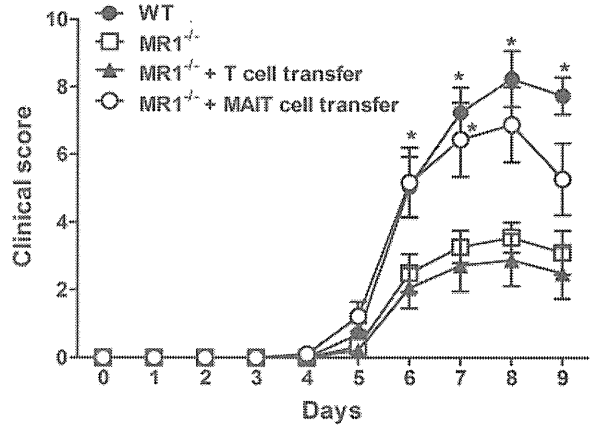

Figure 4. Augmentation of arthritis by adoptive transfer of mucosal-associated invariant T (MAIT) cells in $MR1^{-/-}$ mice. $MR1^{-/-}$ C57BL/6J mice received 5×10^5 NK1.1+TCRβ+ T cells (MAIT cells) or an equal number of NK1.1–TCRβ+ cells (T cells) from V_α19-transgenic $CD1d1^{-/-}$ mice. One day later, collagen antibody–induced arthritis was induced in wild-type (WT) C57BL/6J mice, $MR1^{-/-}$ C57BL/6J mice, and $MR1^{-/-}$ C57BL/6J mice reconstituted with T cells or MAIT cells. Results pooled from 2 similar experiments performed are shown. Values are the mean ± SEM of 8–10 mice per group. * = $P < 0.05$ versus $MR1^{-/-}$ C57BL/6J mice.

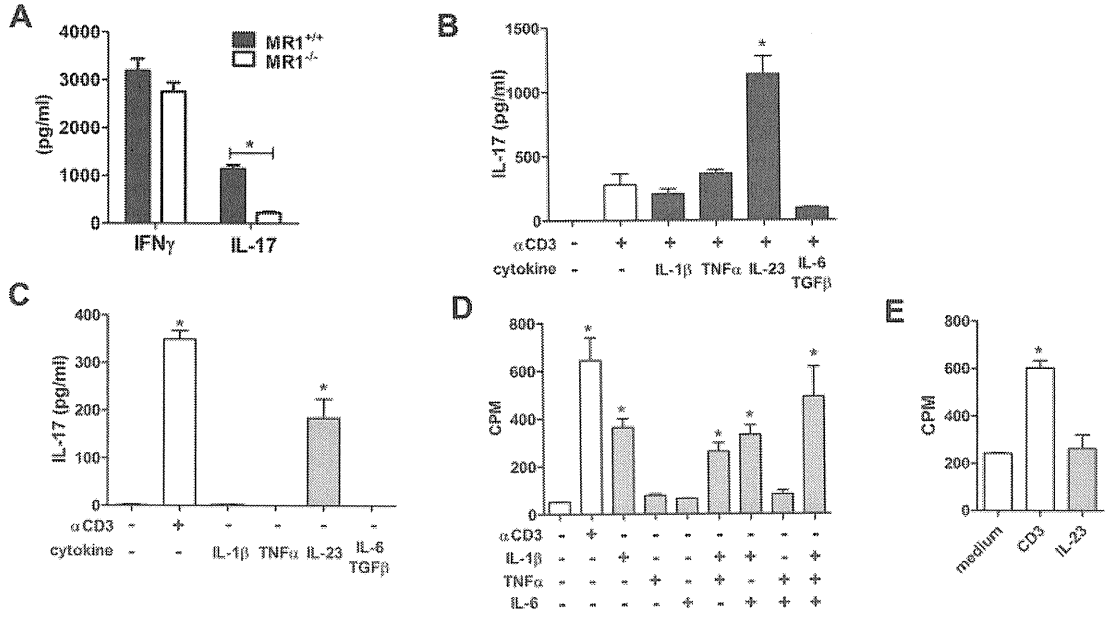

Figure 5. Cytokine-mediated mucosal-associated invariant T (MAIT) cell activation. A, Liver mononuclear cells from $MR1^{+/+}$ C57BL/6J mice and $MR1^{-/-}$ C57BL/6J mice were stimulated for 48 hours with immobilized anti-CD3 (αCD3) monoclonal antibody (mAb). The levels of interferon-γ (IFNγ) and interleukin-17 (IL-17) in culture supernatants were measured by enzyme-linked immunosorbent assay (ELISA). * = $P < 0.05$. B, MAIT cells were stimulated for 48 hours with immobilized anti-CD3 mAb, with or without IL-1β, tumor necrosis factor α (TNFα), IL-23, or IL-6 plus transforming growth factor β (TGFβ), and the levels of IL-17 were measured by ELISA. * = $P < 0.05$ versus anti-CD3 mAb stimulation alone. C, MAIT cells were stimulated with immobilized anti-CD3 mAb or the indicated cytokines, and IL-17 levels were measured. * = $P < 0.05$ versus unstimulated control. D and E, Proliferative responses after 48 hours of exposure to the indicated cytokines were determined as the uptake of ^{3}H-thymidine. Results from a single representative experiment of 2 similar experiments performed are shown. * = $P < 0.05$ versus unstimulated control. Values in A–E are the mean ± SEM.

CAIA model, we performed adoptive transfer experiments. Most NK1.1+ TCRβ T cells within liver lymphocytes from $CD1d1^{+/+}$ mice are iNKT cells, and we and other investigators previously demonstrated that the NK1.1+ TCRβ T cell population in V_α19i-transgenic $CD1d1^{-/-}$ mice is highly enriched in V_α19i TCR+ cells (15,17). Thus, to obtain MAIT cells, we isolated NK1.1+ TCRβ T cells from V_α19i-transgenic $CD1d1^{-/-}$ mice. We adoptively transferred these MAIT cells into $MR1^{-/-}$ C57BL/6J mice, and 1 day later, we injected these mice with anti-CII mAb to induce CAIA. $MR1^{-/-}$ C57BL/6J mice reconstituted with MAIT cells developed severe arthritis at a level similar to that of wild-type (WT) C57BL/6J mice (Figure 4). However, the transfer of an equal number of T cells into $MR1^{-/-}$ C57BL/6J mice had little effect on the clinical arthritis scores. Taken together, these results suggest that the presence of MAIT cells augmented arthritis mainly by enhancing the inflammation in arthritis.

Cytokine-mediated MAIT cell activation. To understand the mechanism by which MAIT cells exacerbate the disease course of arthritis, we first compared the cytokine-producing capacity of T cells from $MR1^{-/-}$ and WT C57BL/6J mice. Upon anti-CD3 mAb stimulation, LMNCs from $MR1^{-/-}$ and WT C57BL/6J mice produced comparable amounts of IFNγ. However, the level of IL-17 was lower in $MR1^{-/-}$ C57BL/6J mice than in WT C57BL/6J mice (Figure 5A).

It was recently demonstrated that human MAIT cells express the Th17-associated transcription factor retinoic acid receptor–related orphan nuclear receptor (ROR) and produce high levels of IL-17 (33). We therefore sought to determine whether mouse MAIT cells produce IL-17, which is known to play a pathogenic role in arthritis. MAIT cells were sorted from LMNCs obtained from V_α19i-transgenic $CD1d1^{-/-}$ mice and were stimulated ex vivo with anti-CD3 mAb. As previously shown (34), MAIT cells produced large amounts of IL-17. In addition, IL-17 production by anti-CD3 mAb–stimulated MAIT cells was augmented in the presence of IL-23 (Figure 5B).

Innate-like lymphocytes such as iNKT cells and

γ/δ T cells are known to be activated by cytokines directly, without TCR stimulation. A combination of IL-12 and IL-18 activates iNKT cells to produce IFNγ, and IL-1 together with IL-23 induces IL-17 production by γ/δ T cells (31,35,36). We therefore next asked whether MAIT cells are activated directly by cytokines. MAIT cells were incubated with various cytokines without TCR stimulation, and cytokine concentrations in the culture supernatants were evaluated. Surprisingly, MAIT cells produced high levels of IL-17 after exposure to IL-23 in the absence of TCR stimulation (Figure 5C).

Inflammatory cytokines such as IL-1β, TNFα, and IL-6 play critical roles in arthritis models and in human RA. Therefore, we next tested whether MAIT cells could be activated by these cytokines. As shown in Figure 5D, IL-1β induced robust proliferation of MAIT cells, although cytokine production was not observed after exposure to these cytokines, including IL-1β (data not shown). In addition, IL-23 did not induce proliferation of MAIT cells (Figure 5E). Thus, in the absence of TCR stimuli, IL-1β induced the proliferation of MAIT cells and IL-23 promoted the production of IL-17 by MAIT cells.

DISCUSSION

Previous studies by our group as well as others revealed that iNKT cells play pathogenic roles in CIA and CAIA by inducing a Th1 or Th17 shift of autoimmune T cells and by augmenting the inflammation in arthritis (25–27). In the present study, we demonstrated that MAIT cells contribute to the severity of CIA and CAIA mostly by augmenting joint inflammation during the effector phase of arthritis. $MR1^{-/-}$ mice were originally generated on the 129P2 background. Although $MR1^{-/-}$ mice were backcrossed onto C57BL/6 or DBA/1J, we are not able to exclude the possibility that some residual sequence from the 129P2 mice affects the arthritis susceptibility of $MR1^{-/-}$ C57BL/6 and $MR1^{-/-}$ DBA/1J mice. However, since the reconstitution of MAIT cells induced severe CAIA in $MR1^{-/-}$ C57BL/6 mice, the phenotype observed in $MR1^{-/-}$ mice seems to be dependent on the lack of MAIT cells.

It has been revealed that there are CD1d-restricted T cells that are different from iNKT cells and do not express an invariant TCRα chain ($V_\alpha14$–$J_\alpha18$ in mice and $V_\alpha24$–$J_\alpha18$ in humans). Such CD1d-restricted T cells are called type II NKT cells and possess different functions from iNKT cells. Recently, CD1d-restricted NKT cells, which recognize murine type II collagen peptide 707–721, were reported to suppress CIA (37). It is not known whether there are distinct subsets with different functions among MAIT cells or whether there are other T cells that are restricted by the MR1 molecule. As adoptively transferred $V_\alpha19i$ T cells augmented CAIA in $MR1^{-/-}$ mice, MAIT cells include the population that enhances the inflammation in arthritis.

It was recently shown that IL-17–producing γ/δ T cells were observed in the joints of mice with CIA and that blocking a certain subset of IL-17–producing γ/δ T cells suppressed CIA (29). However, γ/δ T cells have been shown to be dispensable for the development of CIA (38). In addition, anti-CII–specific antibody levels were comparable between γ/δ T cell–deficient and wild-type mice. These findings suggest that MAIT cells and γ/δ T cells share similar roles in arthritis and that both are involved mainly in the effector phase of arthritis. It is known that γ/δ T cells as well as iNKT cells are increased during CIA. Because MAIT cells share similar features with γ/δ T cells and iNKT cells, MAIT cells may also be increased during CIA.

We observed a significant decrease in IL-17 production by LMNCs upon stimulation with anti-CD3 mAb in $MR1^{-/-}$ mice compared to WT control mice. As sorted MAIT cells produced high amounts of IL-17 after anti-CD3 mAb stimulation, the major source of IL-17 responsible for the difference between $MR1^{-/-}$ and WT mice seems to be MAIT cells. Th17 cells and iNKT cells have been shown to produce IL-21, which enhanced IL-17 production or induced proliferation of IL-17–producing cells (39). It is not known whether MAIT cells produce IL-21, but MAIT cells might augment IL-17 production by other LMNCs, including γ/δ T cells, through such mechanisms. Further studies to determine whether MAIT cells regulate γ/δ T cells under both physiologic and pathologic conditions, including in the presence of arthritis, will be of interest.

The frequency of murine γ/δ T cells is 1–5% in blood lymphocytes and 25–60% in gut lymphocytes. Human γ/δ T cells also comprise up to 2–3% of peripheral T cells (9,10). Although the precise frequency of murine MAIT cells is not known, it has been speculated that MAIT cells may comprise up to 10% of double-negative T cells in the gut lamina propria and <2% of double-negative T cells in the mesenteric lymph nodes, indicating that the frequency of murine MAIT cells is much lower than that of mouse γ/δ T cells (15). It has been suggested that γ/δ T cells are the predominant source of IL-17 in the joints of CIA mice, but IL-17–producing γ/δ T cells could not be detected in RA synovial tissue (31). Recently, Martin et al (23) revealed that human MAIT cells can be identified as $V_\alpha7.2+$ $CD161^{high}$ T cells, which are abundant in blood. In addition, human MAIT cells produce IL-17 and express

tissue-homing chemokine receptors (23). An IL-17–producing CD161^{high} T cell population has been described in human arthritic joints (40). Thus, it is possible that MAIT cells rather than γ/δ T cells play a major role in the pathogenesis of human RA.

CD4+ Th17 cells require IL-6/STAT-3 activation for the expression of RORγt, which is a crucial transcription factor for IL-17 production (41). However, some innate-like lymphocyte subsets, such as iNKT cells, γ/δ T cells, and lymphoid tissue–inducer (LTi)–like cells, are known to constitutively express RORγt, IL-1 receptor type I, and IL-23R (42). In addition, these IL-17–producing innate-like lymphocytes, including LTi cells, γ/δ T cells, and iNKT cells, secrete IL-17 when stimulated by IL-23 with or without IL-1β. In this study, we demonstrated cytokine-mediated activation of MAIT cells. MAIT cells produced IL-17 in response to IL-23. Moreover, IL-1β induced proliferation of MAIT cells. Thus, it is possible that MAIT cells may contribute to the disease progression of arthritis through another mechanism in addition to IL-17 production. In adoptive transfer experiments, MAIT cells augmented the disease severity of CAIA in MR1-deficient mice. Thus, this result also indicates that MAIT cell–mediated exacerbation of arthritis may be induced by cytokines, without a requirement for TCR stimulation.

In EAE, disease suppression by MAIT cells was accompanied by a reduction in the production of cytokines, including IFNγ and IL-17, by T cells and increased IL-10 production by B cells. Encephalitogenic T cells play a major role in EAE (43,44). EAE can be induced in naive mice by transferring myelin-reactive T cells. T cell–targeted therapies, including anti–very late activation antigen 4 treatment, have been shown to suppress EAE. Although CIA was reduced in MR1$^{-/-}$ DBA/1J mice, we observed a significant decrease in CII-specific IgG1 antibody levels in these mice as compared with their WT controls in some experiments (data not shown), suggesting the inhibition of Th1 responses by MAIT cells. Therefore, it is still possible that MAIT cells suppress Th1 response during the early induction phase of CIA. MAIT cells may be functionally plastic, and thus exert different functions depending on the pathologic condition. Arthritis involves massive cytokine production due to various types of immune cell activation. Since MAIT cells can be activated by inflammatory cytokines, MAIT cells may contribute to augment the immune response once overt inflammation occurs.

In summary, we have shown that MAIT cells contribute to the progression of arthritis by enhancing the inflammation in CIA and CAIA models. In addition, we demonstrated that MAIT cells could be activated by cytokine stimulation even without TCR stimulation. We and others previously reported that, although iNKT cells play pathogenic roles in arthritis models, modulation of iNKT cell function by ligands successfully suppressed arthritis (45–47). The proportion of human MAIT cells appears to be much higher than that of mouse MAIT cells. Therefore, MAIT cells may play an important pathogenic role in human arthritis and MAIT cell–targeted therapy may hold promise as a new therapeutic intervention for arthritis, including RA.

ACKNOWLEDGMENTS

The authors thank S. Gilfillan (Washington University School of Medicine, St. Louis, MO) for MR1$^{-/-}$ mice and M. Shimamura (University of Tsukuba, Ibaraki, Japan) for $V_{\alpha}19$-transgenic mice.

AUTHOR CONTRIBUTIONS

All authors were involved in drafting the article or revising it critically for important intellectual content, and all authors approved the final version to be published. Dr. Miyake had full access to all of the data in the study and takes responsibility for the integrity of the data and the accuracy of the data analysis.

Study conception and design. Chiba, Tajima, Miyazaki, Miyake.
Acquisition of data. Chiba, Tajima, Tomi, Miyazaki.
Analysis and interpretation of data. Chiba, Tajima, Tomi, Miyazaki, Yamamura, Miyake.

REFERENCES

1. Chervonsky AV. Influence of microbial environment on autoimmunity [review]. Nat Immunol 2010;11:28–35.
2. Vaahtovuo J, Munukka E, Korkeamaki M, Luukkainen R, Toivanen P. Fecal microbiota in early rheumatoid arthritis. J Rheumatol 2008;35:1500–5.
3. Stone M, Fortin PR, Pacheco-Tena C, Inman RD. Should tetracycline treatment be used more extensively for rheumatoid arthritis? Metaanalysis demonstrates clinical benefit with reduction in disease activity. J Rheumatol 2003;30:2112–22.
4. Nieuwenhuis EE, Visser MR, Kavelaars A, Cobelens PM, Fleer A, Harmsen W, et al. Oral antibiotics as a novel therapy for arthritis: evidence for a beneficial effect of intestinal Escherichia coli. Arthritis Rheum 2000;43:2583–9.
5. Wu HJ, Ivanov II, Darce J, Hattori K, Shima T, Umesaki Y, et al. Gut-residing segmented filamentous bacteria drive autoimmune arthritis via T helper 17 cells. Immunity 2010;32:815–27.
6. Vivier E, Tomasello E, Baratin M, Walzer T, Ugolini S. Functions of natural killer cells [review]. Nat Immunol 2008;9:503–10.
7. Kronenberg M, Kinjo Y. Innate-like recognition of microbes by invariant natural killer T cells [review]. Curr Opin Immunol 2009;21:391–6.
8. Brigl M, Brenner MB. How invariant natural killer T cells respond to infection by recognizing microbial or endogenous lipid antigens [review]. Semin Immunol 2010;22:79–86.
9. Carding SR, Egan PJ. γδ T cells: functional plasticity and heterogeneity [review]. Nat Rev Immunol 2002;2:336–45.
10. Bonneville M, O'Brien RL, Born WK. γδ T cell effector functions: a blend of innate programming and acquired plasticity [review]. Nat Rev Immunol 2010;10:467–78.
11. Allman D, Pillai S. Peripheral B cell subsets [review]. Curr Opin Immunol 2008;20:149–57.

12. Lopes-Carvalho T, Foote J, Kearney JF. Marginal zone B cells in lymphocyte activation and regulation [review]. Curr Opin Immunol 2005;17:244–50.
13. Le Bourhis L, Guerri L, Dusseaux M, Martin E, Soudais C, Lantz O. Mucosal-associated invariant T cells: unconventional development and function [review]. Trends Immunol 2011;32:212–8.
14. Treiner E, Duban L, Bahram S, Radosavljevic M, Wanner V, Tilloy F, et al. Selection of evolutionarily conserved mucosal-associated invariant T cells by MR1. Nature 2003;422:164–9.
15. Kawachi I, Maldonado J, Strader C, Gilfillan S. MR1-restricted Vα19i mucosal-associated invariant T cells are innate T cells in the gut lamina propria that provide a rapid and diverse cytokine response. J Immunol 2006;176:1618–27.
16. Illes Z, Shimamura M, Newcombe J, Oka N, Yamamura T. Accumulation of Vα7.2-Jα33 invariant T cells in human autoimmune inflammatory lesions in the nervous system. Int Immunol 2004;16:223–30.
17. Croxford JL, Miyake S, Huang YY, Shimamura M, Yamamura T. Invariant Vα19i T cells regulate autoimmune inflammation. Nat Immunol 2006;7:987–94.
18. Peterfalvi A, Gomori E, Magyarlaki T, Pal J, Banati M, Javorhazy A, et al. Invariant Vα7.2-Jα33 TCR is expressed in human kidney and brain tumors indicating infiltration by mucosal-associated invariant T (MAIT) cells. Int Immunol 2008;20:1517–25.
19. Gold MC, Cerri S, Smyk-Pearson S, Cansler ME, Vogt TM, Delepine J, et al. Human mucosal associated invariant T cells detect bacterially infected cells. PLoS Biol 2010;8:e1000407.
20. Le Bourhis L, Martin E, Peguillet I, Guihot A, Froux N, Core M, et al. Antimicrobial activity of mucosal-associated invariant T cells. Nat Immunol 2010;11:701–8.
21. Tilloy F, Treiner E, Park SH, Garcia C, Lemonnier F, de la Salle H, et al. An invariant T cell receptor α chain defines a novel TAP-independent major histocompatibility complex class IB-restricted α/β T cell subpopulation in mammals. J Exp Med 1999; 189:1907–21.
22. Lantz O, Bendelac A. An invariant T cell receptor α chain is used by a unique subset of major histocompatibility complex class I-specific CD4+ and CD4−CD8− T cells in mice and humans. J Exp Med 1994;180:1097–106.
23. Martin E, Treiner E, Duban L, Guerri L, Laude H, Toly C, et al. Stepwise development of MAIT cells in mouse and human. PLoS Biol 2009;7:e54.
24. Lo CK, Lam QL, Sun L, Wang S, Ko KH, Xu H, et al. Natural killer cell degeneration exacerbates experimental arthritis in mice via enhanced interleukin-17 production. Arthritis Rheum 2008;58: 2700–11.
25. Chiba A, Kaieda S, Oki S, Yamamura T, Miyake S. The involvement of $V_{\alpha}14$ natural killer T cells in the pathogenesis of arthritis in murine models. Arthritis Rheum 2005;52:1941–8.
26. Kim HY, Kim HJ, Min HS, Kim S, Park WS, Park SH, et al. NKT cells promote antibody-induced joint inflammation by suppressing transforming growth factor β1 production. J Exp Med 2005;201: 41–7.
27. Ohnishi Y, Tsutsumi A, Goto D, Itoh S, Matsumoto I, Taniguchi M, et al. TCR Vα14 natural killer T cells function as effector T cells in mice with collagen-induced arthritis. Clin Exp Immunol 2005;141:47–53.
28. Teige A, Bockermann R, Hasan M, Olofsson KE, Liu Y, Issazadeh-Navikas S. CD1d-dependent NKT cells play a protective role in acute and chronic arthritis models by ameliorating antigen-specific Th1 responses. J Immunol 2010;185:345–56.
29. Roark CL, French JD, Taylor MA, Bendele AM, Born WK, O'Brien RL. Exacerbation of collagen-induced arthritis by oligoclonal, IL-17-producing γδ T cells. J Immunol 2007;179:5576–83.
30. Peterman GM, Spencer C, Sperling AI, Bluestone JA. Role of γδ T cells in murine collagen-induced arthritis. J Immunol 1993;151: 6546–58.
31. Ito Y, Usui T, Kobayashi S, Iguchi-Hashimoto M, Ito H, Yoshitomi H, et al. Gamma/delta T cells are the predominant source of interleukin-17 in affected joints in collagen-induced arthritis, but not in rheumatoid arthritis. Arthritis Rheum 2009;60:2294–303.
32. Okamoto N, Kanie O, Huang YY, Fujii R, Watanabe H, Shimamura M. Synthetic α-mannosyl ceramide as a potent stimulant for an NKT cell repertoire bearing the invariant Vα19-Jα26 TCR α chain. Chem Biol 2005;12:677–83.
33. Dusseaux M, Martin E, Serriari N, Peguillet I, Premel V, Louis D, et al. Human MAIT cells are xenobiotic-resistant, tissue-targeted, $CD161^{hi}$ IL-17-secreting T cells. Blood 2011;117:1250–9.
34. Shimamura M, Huang YY, Kobayashi M, Goji H. Altered production of immunoregulatory cytokines by invariant Vα19 TCR-bearing cells dependent on the duration and intensity of TCR engagement. Int Immunol 2009;21:179–85.
35. Nagarajan NA, Kronenberg M. Invariant NKT cells amplify the innate immune response to lipopolysaccharide. J Immunol 2007; 178:2706-13.
36. Sutton CE, Lalor SJ, Sweeney CM, Brereton CF, Lavelle EC, Mills KH. Interleukin-1 and IL-23 induce innate IL-17 production from γδ T cells, amplifying Th17 responses and autoimmunity. Immunity 2009;31:331–41.
37. Liu Y, Teige A, Mondoc E, Ibrahim S, Holmdahl R, Issazadeh-Navikas S. Endogenous collagen peptide activation of CD1d-restricted NKT cells ameliorates tissue-specific inflammation in mice. J Clin Invest 2011;121:249–64.
38. Corthay A, Johansson A, Vestberg M, Holmdahl R. Collagen-induced arthritis development requires αβT cells but not γδ T cells: studies with T cell-deficient (TCR mutant) mice. Int Immunol 1999;11:1065–73.
39. Spolski R, Leonard WJ. Interleukin-21: basic biology and implications for cancer and autoimmunity [review]. Annu Rev Immunol 2008;26:57–79.
40. Billerbeck E, Kang YH, Walker L, Lockstone H, Grafmueller S, Fleming V, et al. Analysis of CD161 expression on human CD8+ T cells defines a distinct functional subset with tissue-homing properties. Proc Natl Acad Sci U S A 2010;107:3006–11.
41. Zhu J, Yamane H, Paul WE. Differentiation of effector CD4 T cell populations [review]. Annu Rev Immunol 2010:445–89.
42. Cua DJ, Tato CM. Innate IL-17–producing cells: the sentinels of the immune system [review]. Nat Rev Immunol 2010;10:479–89.
43. Wekerle H. Lessons from multiple sclerosis: models, concepts, observations [review]. Ann Rheum Dis 2008;67 Suppl III:iii56–60.
44. Fletcher JM, Lalor SJ, Sewwney CM, Tubridy N, Mills KH. T cells in multiple sclerosis and experimental autoimmune encephalomyelitis [review]. Clin Exp Immunol 2010;162:1–11.
45. Chiba A, Oki S, Miyamoto K, Hashimoto H, Yamamura T, Miyake S. Suppression of collagen-induced arthritis by natural killer T cell activation with OCH, a sphingosine-truncated analog of α-galactosylceramide. Arthritis Rheum 2004;50:305–13.
46. Coppieters K, Van Beneden K, Jacques P, Dewint P, Vervloet A, Vander Cruyssen B, et al. A single early activation of invariant NK T cells confers long-term protection against collagen-induced arthritis in a ligand-specific manner. J Immunol 2007;179:2300–9.
47. Kaieda S, Tomi C, Oki S, Yamamura T, Miyake S. Activation of invariant natural killer T cells by synthetic glycolipid ligands suppresses autoantibody-induced arthritis. Arthritis Rheum 2007; 56:1836–45.

PLoS one

Type II NKT Cells Stimulate Diet-Induced Obesity by Mediating Adipose Tissue Inflammation, Steatohepatitis and Insulin Resistance

Masashi Satoh[1,2☯], Yasuhiro Andoh[2,3☯], Christopher Stuart Clingan[2,4], Hisako Ogura[2], Satoshi Fujii[5], Koji Eshima[1], Toshinori Nakayama[6], Masaru Taniguchi[7], Noriyuki Hirata[2,8], Naoki Ishimori[3], Hiroyuki Tsutsui[3], Kazunori Onoé[2], Kazuya Iwabuchi[1,2]*

1 Department of Immunology, Kitasato University School of Medicine, Sagamihar, Japan, **2** Division of Immunobiology, Research Section of Pathophysiology, Institute for Genetic Medicine, Hokkaido University, Sapporo, Japan, **3** Department of Cardiovascular Medicine, Hokkaido University Graduate School of Medicine, Sapporo, Japan, **4** Department of Microbiology and Immunology, Vanderbilt University School of Medicine, Nashville, Tennessee, United States of America, **5** Department of Molecular and Cellular Pathobiology and Therapeutics, Graduate School of Pharmaceutical Sciences, Nagoya City University, Nagoya, Japan, **6** Department of Immunology, Graduate School of Medicine, Chiba University, Chiba, Japan, **7** RIKEN Research Center for Allergy and Immunology, Yokohama, Japan, **8** Division of Cancer Biology, Research Section of Pathophysiology, Institute for Genetic Medicine, Hokkaido University, Sapporo, Japan

Abstract

The progression of obesity is accompanied by a chronic inflammatory process that involves both innate and acquired immunity. Natural killer T (NKT) cells recognize lipid antigens and are also distributed in adipose tissue. To examine the involvement of NKT cells in the development of obesity, C57BL/6 mice (wild type; WT), and two NKT-cell-deficient strains, Jα18$^{-/-}$ mice that lack the type I subset and CD1d$^{-/-}$ mice that lack both the type I and II subsets, were fed a high fat diet (HFD). CD1d$^{-/-}$ mice gained the least body weight with the least weight in perigonadal and brown adipose tissue as well as in the liver, compared to WT or Jα18$^{-/-}$ mice fed an HFD. Histologically, CD1d$^{-/-}$ mice had significantly smaller adipocytes and developed significantly milder hepatosteatosis than WT or Jα18$^{-/-}$ mice. The number of NK1.1^{+}TCRβ^{+} cells in adipose tissue increased when WT mice were fed an HFD and were mostly invariant Vα14Jα18-negative. CD11b^{+} macrophages (Mϕ) were another major subset of cells in adipose tissue infiltrates, and they were divided into F4/80^{high} and F4/80^{low} cells. The F4/80^{low}-Mϕ subset in adipose tissue was increased in CD1d$^{-/-}$ mice, and this population likely played an anti-inflammatory role. Glucose intolerance and insulin resistance in CD1d$^{-/-}$ mice were not aggravated as in WT or Jα18$^{-/-}$ mice fed an HFD, likely due to a lower grade of inflammation and adiposity. Collectively, our findings provide evidence that type II NKT cells initiate inflammation in the liver and adipose tissue and exacerbate the course of obesity that leads to insulin resistance.

Citation: Satoh M, Andoh Y, Clingan CS, Ogura H, Fujii S, et al. (2012) Type II NKT Cells Stimulate Diet-Induced Obesity by Mediating Adipose Tissue Inflammation, Steatohepatitis and Insulin Resistance. PLoS ONE 7(2): e30568. doi:10.1371/journal.pone.0030568

Editor: Simon Afford, University of Birmingham, United Kingdom

Received August 9, 2011; **Accepted** December 19, 2011; **Published** February 22, 2012

Funding: This work was supported in part by Grant-in-Aid for Scientific Research (#B: #20390106) by the Japan Society for the Promotion of Science (JSPS), Global COE Program, Establishment of International Collaboration Center for Zoonosis Control, by the Ministry of Education, Culture, Sports, Science, and Technology (MEXT) of Japan, a Health and Labor Sciences Research Grant on Intractable Diseases (Neuroimmunological Diseases) from the Ministry of Health, Labor and Welfare of Japan, and a Grant by Heisei Ijuku Tomakomai East Hospital. MS is a recipient of a Parent's Association (Keyaki Kai) Grant of Kitasa to University School of Medicine. No additional external funding received for this study. The funders had no role in study design, data collection and analysis, decision to publish, or preparation of the manuscript.

Competing Interests: The authors have declared that no competing interests exist.

* E-mail: akimari@kitasato-u.ac.jp

☯ These authors contributed equally to this work.

Introduction

Obesity is thought to progress with caloric excess under a chronic inflammatory process characterized by infiltration of adipose tissue by Mϕ and by cells of the adaptive immune system, such as T cells [1–3]. The inflammation in adipose tissue induces alterations in metabolic and endocrine functions of adipocytes, which leads to insulin resistance and various pathological responses [4,5]. Recent studies by Nishimura et al revealed the active participation of CD8^{+} T cells in chronic inflammation in adipose tissue [6]. Moreover, CD4^{+}Foxp3^{+} T cells with unique specificity have been detected in adipose tissue and were suggested to regulate the development of obesity by suppressing inflammatory responses [7]. Furthermore, additional findings showed that the transfer of CD4^{+} T cells from WT but not from T-cell receptor transgenic mice ameliorated the metabolic dysregulation in Rag-1$^{-/-}$ mice fed a high fat diet (HFD), which led to the idea that CD4^{+} T cells play a suppressive role in diet-induced obesity (DIO) [8]. These studies have indicated that T cells that infiltrate adipose tissue are not just inert bystanders but are active modifiers of inflammation and thus either aggravate or ameliorate obesity.

Natural killer T (NKT) cells are a unique subset of T-lineage cells that recognize various lipid antigens in the context of CD1d molecules [9]. Among lipid ligands, α-galactosylceramide (α-GalCer) is the prototype ligand [10] that can stimulate NKT cells to promptly produce large amounts of various cytokines and chemokines and also demonstrate cytocidal activity [11]. Endogenous ligands can also stimulate NKT cells to perform their innate

effector functions [12]. Moreover, NKT cells localize to the liver [13], where lipid metabolism is active, and in adipose tissue [14], another location for lipid metabolism with endocrine functions. These considerations led us to suggest that, NKT cells might play a role in a disease that involves abnormal lipid metabolism or lipid-related inflammation. Indeed, several research groups including our team have demonstrated that NKT cells accelerate atherogenesis in a mouse model of atherosclerosis [15–17]. Furthermore, we have examined the involvement of NKT cells in insulin resistance induced in mice fed an HFD and demonstrated that NKT cells play an important role in adipose-tissue inflammation and glucose intolerance in β_2-microglobulin knockout ($\beta_2m^{-/-}$) mice with DIO [18]. However, both mainstream $CD8^+$ T cells and various innate lymphocytes other than NKT cells also are absent in $\beta_2m^{-/-}$ mice [19]. Thus, we attempted to examine the involvement of NKT cells in DIO and insulin resistance using NKT cell-deficient mice. To this end, we compared B6 (WT) and two strains of NKT cell-deficient mice, $CD1d^{-/-}$ and $J\alpha18^{-/-}$ mice on a B6 genetic background. Unlike our previous study in $\beta_2m^{-/-}$ mice [18], DIO was significantly suppressed in $CD1d^{-/-}$ mice compared to WT mice. Moreover, in $J\alpha18^{-/-}$ mice where type I but not type II NKT cells were deficient, DIO was induced to an equal extent as in WT mice. The possible mechanisms underlying lipid-induced NKT-cell activation and the development of chronic inflammation by type II NKT cells in DIO are discussed.

Materials and Methods

Mice

Male and female 8-week-old C57BL/6 (B6; Nippon SLC, Shizuoka, Japan), B6.$CD1d^{-/-}$ [20], and B6.$J\alpha18^{-/-}$ [21] mice were used. Mice were maintained on food and water *ad libitum* until they reached the desired weight (20–24 g) or age (8 wk) under specific pathogen-free conditions. All experiments were approved by the Committees of Animal Experimentation at Hokkaido University (permit number: #09-0022) and Kitasato University (permit number: #2011 105).

Diet-induced obesity

Mice were fed either regular chow as a standard fat diet (SFD; Nihon Nosan: fat 4.3%, cholesterol 0.03%, protein 18.3%, carbohydrate 58.3%) or an HFD (CLEA Japan HFD-32: fat (powdered tallow and safflower oil of high oleic type) 32.0%, protein 25.5%, fiber 2.9%, mineral 4.0%, nitrogen 29.4%, water 6.2%) starting from 8 wk of age for 18 wk. Mice were weighed weekly. The ingredients of HFD-32 are listed in detail at <http://www.clea-japan.com/Feed/pdf/clea_hfd32.pdf>. Major fatty acids included oleic acid ($C_{18:1}$; 64.3%), palmitic acid ($C_{16:0}$; 12.6%), linoleic acid ($C_{18:2}$; 10.2%), and stearic acid ($C_{18:0}$; 7.5%). After 18 wk of feeding, mice were sacrificed for analysis. For some experiments, mice were injected intraperitoneally with α-GalCer (0.1 μg/g body weight, BW) or vehicle as control to examine the change of BW.

Blood chemistry

Total cholesterol (T-chol), high-density lipoprotein (HDL) cholesterol (HDL-chol), triglyceride (TG), and alanine aminotransferase (ALT) concentrations in sera were quantified by colorimetric assays with the Fuji Drychem system (Fujifilm Medical, Osaka, Japan) according to the manufacturer's protocol, as described elsewhere [16].

Histology and quantitative analyses of microscopic images

Perigonadal fat tissue was removed and fixed with buffered formaldehyde solution (10%) followed by ordinary processing for paraffin-embedded sections and hematoxylin-eosin (HE) staining. Images of the HE-stained adipose tissue were incorporated with a BIOREVO microscope (BZ8100; Keyence Corp., Osaka, Japan), and morphometric analyses were performed with image analysis software (BZ-H2A, -H1C) equipped on the microscope. Liver samples were snap-frozen in OCT compound (Sakura Finetek Co., Tokyo, Japan) with liquid nitrogen, and cryosections were stained with Oil Red O (ORO) (Sigma Chemical Co., St. Louis, MO) and Meyer's hematoxylin (Wako Pure Chemical Co. Ltd., Osaka, Japan). Images of lipid droplets in hepatocytes stained red were quantified by computerized image analysis system (Scion Image software, Scion Corp., Frederick, MD).

Flow cytometry

Splenocytes were prepared by mincing the spleen with a glass homogenizer, and red blood cells were lysed with Tris-NH_4Cl solution. Hepatic mononuclear cells (HMNC) were isolated from liver homogenates by density-gradient centrifugation with 33% Percoll™ (GE Healthcare Life Sciences, Piscataway, NJ) as previously reported [22]. Stromal vascular cells were isolated from the digest of perigonadal fat by mincing and incubating with collagenase D solution (2 mg/ml) (Roche Diagnostics, Indianapolis, IN) for 1–1.5 h. The cells were incubated with 2.4G2 monoclonal antibody (mAb) (anti-FcγRIII/II) to block non-specific binding of primary mAb and then reacted with CD1d:Ig recombinant fusion protein (BD Biosciences Pharmingen, San Diego, CA) loaded with α-GalCer (α-GalCer-CD1d-dimer), followed by detection with phycoerythrin (PE)-conjugated anti-mouse IgG_1 mAb (A85-1; BD) according to the manufacturer's protocol [16]. After washing, cells were stained with a combination of the following mAb conjugates: fluorescein isothiocyanate (FITC)-anti-TCRβ chain (H57-597; BD), -anti-CD3ε (145-2C11; BD), -anti-CD1d (1B1; BD), -anti-CD206 (MR5D3; BioLegend, San Diego, CA), -rat IgG_{2a} (BD), -rat IgG_{2b} (BD), allophycocyanin (APC)-anti-NK1.1 (PK136; BD, BioLegend), -anti-CD11c (HL3; BD), -Streptavidin (BioLegend), PE-anti-CD4 (RM4-5; BD), -anti-CD8 (53-6.7; BD), -anti-CD11b (M1/70; BioLegend), and APC-Cy7-Streptavidin (BD). Stained cells were acquired with FACS Calibur or Canto II flow cytometers (BD Bioscience Immunocytometry Systems, San Jose, CA) and analyzed with CellQuest, FACS Diva (BDIS), or FlowJo (Tommy Digital Biology, Tokyo, Japan) software as described elsewhere [16]. Propidium iodide (PI; Sigma) or 7-aminoactinomycin D (7-AAD; BD) positive cells were electronically gated as dead cells from the analysis.

Quantification of serum cytokines and adipokines

The concentration of Th1/Th2 and inflammatory cytokines, including IFN-γ, tumor necrosis factor (TNF)-α, IL-1α, 2, 4, 5, 6, 10, 17, and GM-CSF in serum was quantified with Mouse Th1/Th2 10plex FlowCytomix™ Multiplex (Bender MedSystems GmbH, Vienna, Austria) according to the manufacturer's protocol with a flow cytometer. Leptin (Morinaga Institute of Biological Sciences, Kanagawa, Japan) in sera was respectively quantified with enzyme-linked immunosorbent assay (ELISA) kit according to the manufacturers' protocol.

IPGTT and insulin tolerance test

Intraperitoneal (*i.p.*) glucose tolerance test (IPGTT) was performed by *i.p.* injection of glucose solution (1 g/kg) after 16 h of fasting [6]. The insulin tolerance test (ITT) was performed by *i.p.* injection of insulin (0.751U/kg; Humulin R 100 U/ml; Eli Lilly Japan KK, Kobe, Japan) after 3.5 h of fasting. The blood glucose level was serially quantified with a blood glucose monitor (MEDISAFE MINI; Terumo Corp., Tokyo, Japan). The insulin

level was also quantified with the mouse insulin ELISA kit (Morinaga) according to the manufacturer's protocol.

HMNC transfer

HMNC were obtained from either Jα18$^{-/-}$ or CD1d$^{-/-}$ mice and were intravenously transferred to CD1d$^{-/-}$ recipient mice (1×10^6/mouse) at 8 wk. These mice were fed an HFD for 14 weeks and tested for IPGTT and ITT as above.

Culture of Mφ from the stromal vascular fraction (SVF) of adipose tissue

Cells (1×10^5/well) obtained from perigonadal adipose tissue were cultured in RPMI medium (supplemented with 10% heat-inactivated fetal calf serum, 100 U/ml penicillin, 100 μg/ml streptomycin, and 50 μM β-mercaptoethanol) with 1 μg/ml LPS for 20 h. After 20 h, supernatants were collected and frozen at −80°C, and cytokines were later quantified as described above.

Statistical analysis

Results were demonstrated as means ± standard deviation (s.d.). Statistical analysis between two groups was performed by Student's *t*-test and among three groups was performed using ANOVA followed by Tukey-Kramer tests. Pearson's correlation coefficient test was used to examine the correlation. Values with $P<0.05$ were considered statistically significant.

Results

Impact of the presence of NKT cells on the weight gain of mice fed an HFD

Female or male B6 (WT), B6.Jα18$^{-/-}$ (Jα18$^{-/-}$), and B6.CD1d$^{-/-}$ (CD1d$^{-/-}$) mice were fed either an SFD or an HFD from 8 wk to 22~26 wk of age (for 14~18 wk), and the BW of each group of mice was plotted over time. Three groups of female (Figure 1A) or male (Figure 1B) mice showed a similar and gradual increase of BW when fed an SFD. On the other hand, all groups of female and male mice gained substantially more BW on HFD than those on SFD. However, CD1d$^{-/-}$ mice showed significantly less gains than those of WT and Jα18$^{-/-}$ mice (Figure 1A, B). Consistently, the least difference was observed in CD1d$^{-/-}$ mice when the net gain ([BW on HFD at *n* wk]−[BW on HFD at 8 wk]: n≥8 wk) was compared (Figure 1C, D). We also compared BW in WT mice that received either the prototypical type I NKT cell ligand α-GalCer or vehicle when fed either an SFD or an HFD. There was no significant difference in weight gain between mice that received α-GalCer or vehicle and fed either an SFD or an HFD (Figure S1A), suggesting that type I NKT cells might have a minimal role in the development of DIO even when the activating ligand is provided.

When the daily food intake per animal was compared in each group of mice by calculating Σ[(amounts given−amounts left)/total periods] throughout the feeding periods, CD1d$^{-/-}$ female

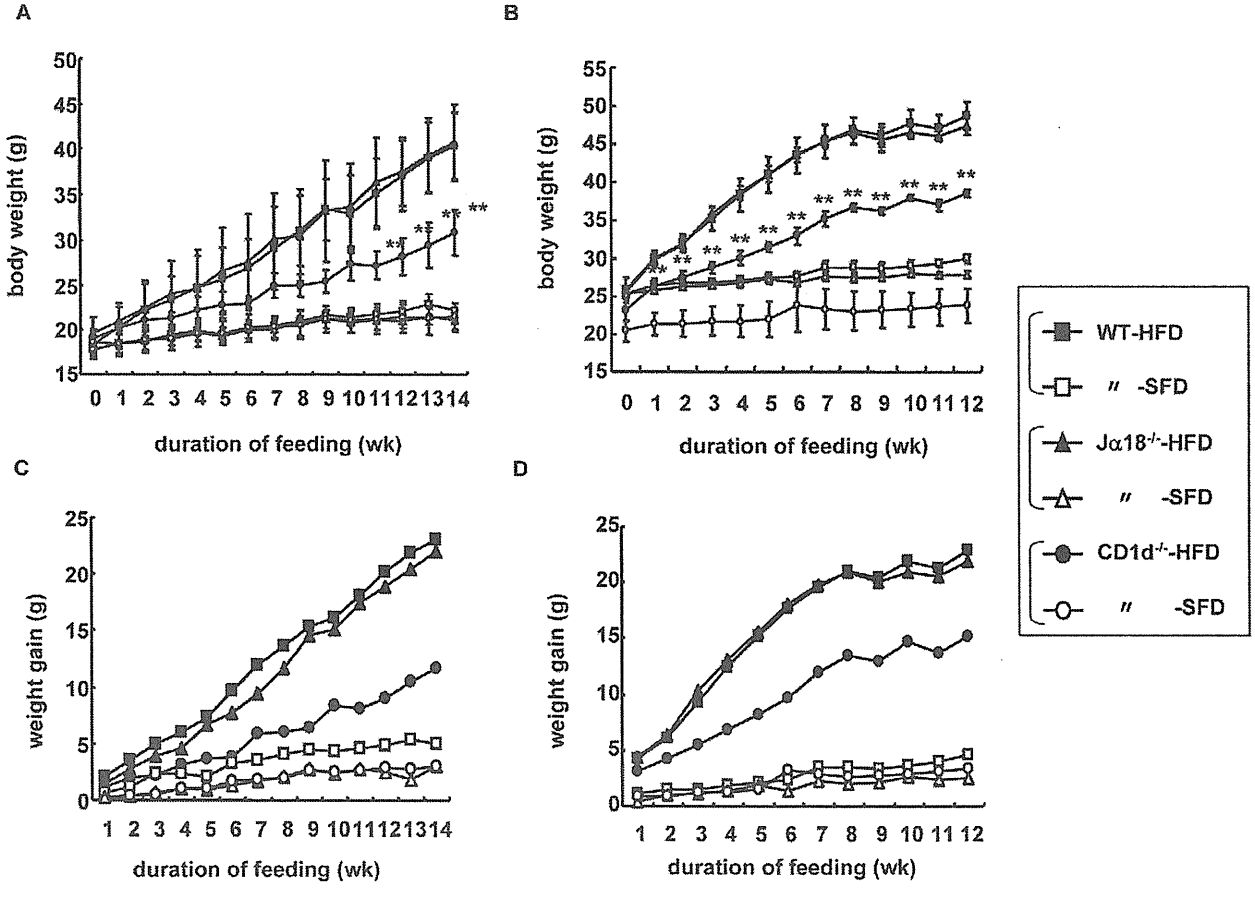

Figure 1. Body weight and weight gain of three strains of mice fed an SFD or an HFD. (A, B) Body weight (BW) of female (A) and male mice (B) fed a high-fat diet (HFD) or a standard-fat diet (SFD) at 8 wk and weighed weekly. (n = 3–7 in each group) (C, D) Representative data of three similar experiments are shown. Weight gain ($\Delta BW = BW_{n\ wk} - BW_{8\ wk}$; n≥9) of female (C) and male (D) mice. Each point represents mean ± standard deviation (s.d.). Statistical analysis was performed according to the Tukey-Kramer test. $^{**}p<0.01$ (WT and Jα18$^{-/-}$ vs CD1d$^{-/-}$).
doi:10.1371/journal.pone.0030568.g001

mice took in slightly smaller amounts of both SFD and HFD than the other two strains, WT and Jα18$^{-/-}$ mice (Figure 2A). A similar tendency in food intake was observed in male mice (data not shown).

The BW of CD1d$^{-/-}$ mice was significantly lower than that of WT and Jα18$^{-/-}$ mice after 18 wk of HFD feeding (Figure 2B) (WT = Jα18$^{-/-}$ > CD1d$^{-/-}$; $p<0.01$ between WT and CD1d$^{-/-}$; Jα18$^{-/-}$ and CD1d$^{-/-}$). The difference in BW in each group of mice was attributable to the sum of the differences in weights of organs and tissues. Thus, the liver, perigonadal fat tissue (white adipose tissue; WAT) and fat tissue between the scapulae (brown adipose tissue; BAT) of each group were obtained and compared. Consistent with the differences in BW, CD1d$^{-/-}$ mice had lower liver weight (Figure 2C) (WT = Jα18$^{-/-}$ > CD1d$^{-/-}$; $p<0.01$ between WT and CD1d$^{-/-}$; $p<0.05$ between Jα18$^{-/-}$ and CD1d$^{-/-}$), lower WAT weight (Figure 2D) (WT ≥ Jα18$^{-/-}$ > CD1d$^{-/-}$; $p<0.01$ between WT and CD1d$^{-/-}$; Jα18$^{-/-}$ and CD1d$^{-/-}$) and lower BAT weight (Figure 2E) (WT ≥ Jα18$^{-/-}$ > CD1d$^{-/-}$; $p<0.01$ between WT and CD1d$^{-/-}$), when compared to those of sex-matched WT or Jα18$^{-/-}$ mice fed an HFD (closed bar). In SFD-fed mice, there were no significant differences in the weights of the whole BW, liver, WAT, and BAT among the three groups of mice (Figure 2B–E; open bar).

When serum lipids were quantified in the three groups of mice fed an HFD, WT and Jα18$^{-/-}$ mice exhibited significantly higher levels of T-chol- and HDL-chol than CD1d$^{-/-}$ mice (Figure S2A, B). The cholesterol level was consistent with the extent of adiposity, whereas the TG level was not different among the three groups (Figure S2C).

HFD-induced hepatosteatosis and adipocyte hypertrophy are ameliorated in CD1d$^{-/-}$ mice

First, livers were histologically examined for major causes of weight gain among three strains of mice on HFD. WT and Jα18$^{-/-}$ mice on HFD had marked hepatosteatosis, which was revealed by red deposits on ORO staining (Figure 3A). On the other hand, livers of CD1d$^{-/-}$ mice that appeared less fatty exhibited lighter deposits on ORO staining (Figure 3A). The ORO-positive regions in CD1d$^{-/-}$ livers were significantly smaller than those of WT and Jα18$^{-/-}$ mice (Figure 3B). The severity of steatosis appeared consistent with the liver weight and dyslipidemic level in each strain (Figure 2A and B). Furthermore, the ALT level, a marker of liver damage, was significantly suppressed in CD1d$^{-/-}$ mice (Figure 3C). We also quantified pro-inflammatory cytokines that were secreted from HMNC in mice fed an HFD upon stimulation with LPS. Production of IL-6 and TNF-α in culture supernatants was increased in WT and Jα18$^{-/-}$ mice, whereas it was suppressed in HMNC cultures of CD1d$^{-/-}$ mice (Figure 3D, E). Thus, lipid-induced inflammation may be suppressed in the absence of CD1d and CD1d-restricted NKT cells.

Next, we similarly analyzed adipose tissues that also contribute to the difference in BW in the three groups of mice. CD1d$^{-/-}$ mice had apparently smaller adipocytes in adipose tissue even on HFD, whereas enlarged adipocytes occupied the entire tissue in WT and Jα18$^{-/-}$ mice (Figure 4A). Of note, boundaries of adipocytes formed almost straight lines due to the close packing of adipocytes in WT mice (Figure 4A left panel). To compare adipocyte size in WAT of each group of mice, the circumference of

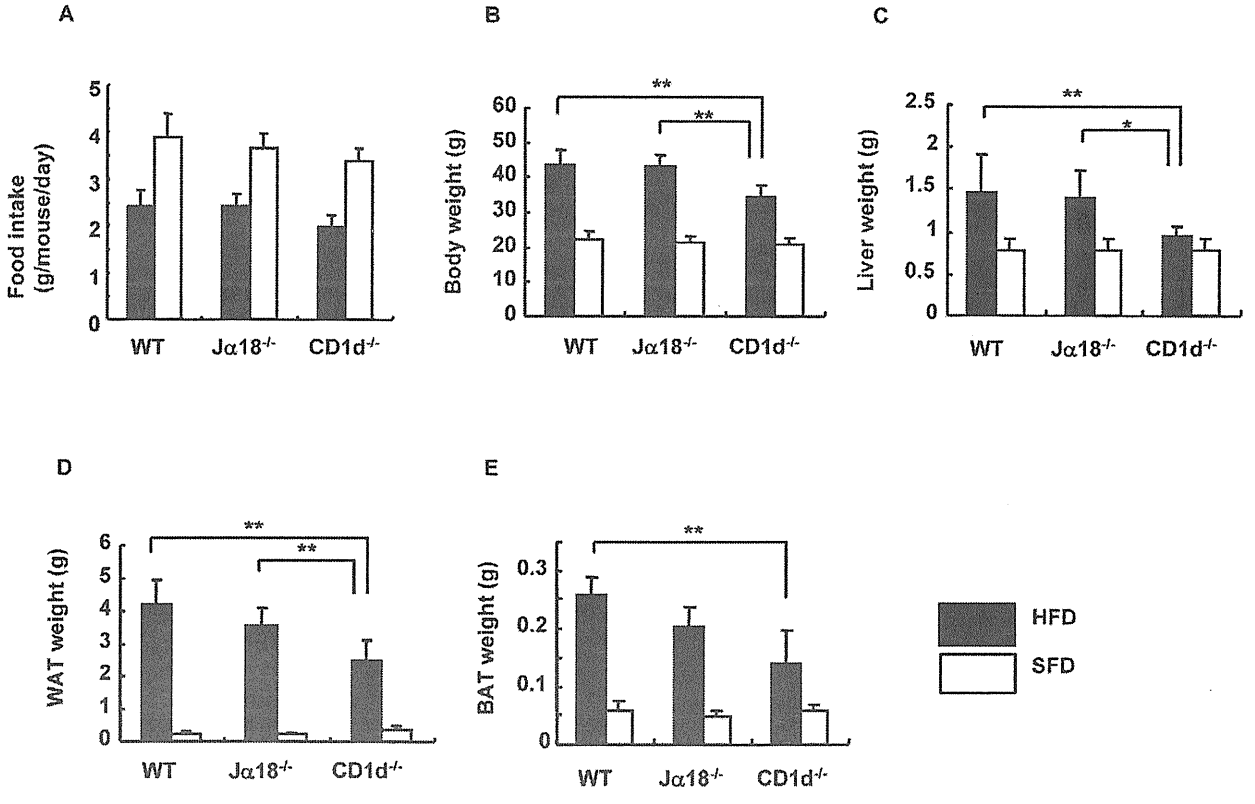

Figure 2. Physiological parameters of three strains of female mice fed an SFD or an HFD. (A) Food intake of mice in each group (g/mouse/day). (B–E) The body, liver, perigonadal adipose tissue (WAT), and brown adipose tissue (BAT) were weighed after 18 wk of feeding at 26 wk of age (n = 3–7 in each group). Representative data of three similar experiments are shown. The results are expressed as mean ± s.d. Statistical analysis was performed according to the Tukey-Kramer test. *$p<0.05$, **$p<0.01$.
doi:10.1371/journal.pone.0030568.g002

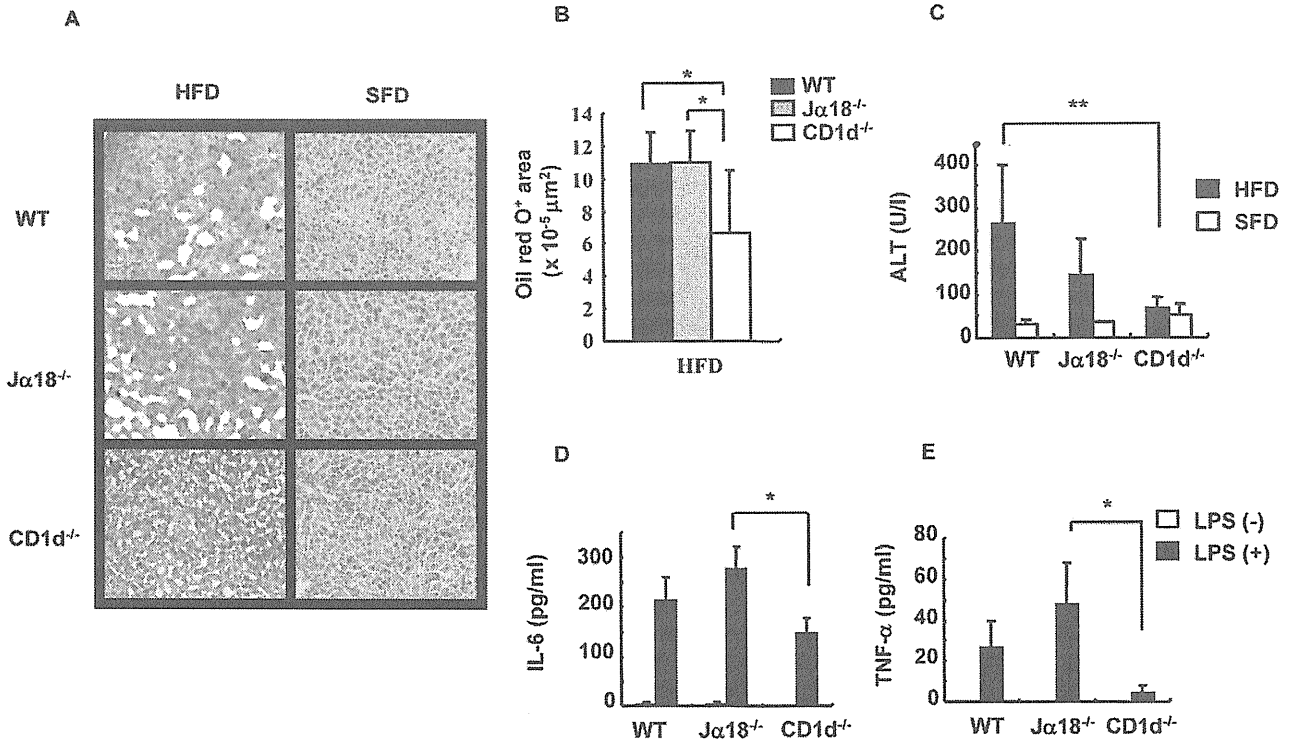

Figure 3. Histology and cytokine production in the liver. (A) A liver section was stained with ORO (frozen section) in SFD- and HFD-fed mice. (B) Red-stained lipid droplets in liver sections of HFD-fed mice were quantified with image analysis software. (C) Serum levels of ALT were quantified with the Drychem system. (D, E) The production of cytokines from HMNC of HFD-fed mice stimulated with LPS for 20 h (n = 3–4 female mice in each group). The results are expressed as mean ± s.d. Statistical analysis was performed according to the Tukey-Kramer test. *$p<0.05$, **$p<0.01$.
doi:10.1371/journal.pone.0030568.g003

each adipocyte was morphometrically compared (Figure 4B). The adipocytes from CD1d$^{-/-}$ mice had significantly smaller circumference than those from WT and Jα18$^{-/-}$ mice.

When leptin is overexpressed, mice demonstrate a lean phenotype [23]. To examine whether CD1d$^{-/-}$ expressed a higher level of leptin in sera than WT and Jα18$^{-/-}$ mice, serum leptin levels were quantified. However, CD1d$^{-/-}$ showed the lowest level among the three strains of mice, which was proportional to the volume of WAT (Figure 4C).

Analysis of infiltrated cellular components in liver of mice fed an HFD

Our findings thus far showed that adiposity and hepatosteatosis were similar between WT and Jα18$^{-/-}$ but were minimal in CD1d$^{-/-}$ mice. The difference between Jα18$^{-/-}$ and CD1d$^{-/-}$ mice is solely the absence of type II NKT cells selected by CD1d in CD1d$^{-/-}$ but not Jα18$^{-/-}$ mice. To study the relationship between type I (iNKT) and type II NKT cells, we analyzed NKT cell subsets in liver and adipose tissue of each strain. As shown in our previous report with the short term feeding of HFD [18], the proportion of NKT cells in liver decreased in WT mice fed an HFD compared to mice on an SFD when the HMNC fraction was stained with a combination of either α-GalCer-loaded CD1d-dimer and anti-TCRβ mAb (iNKT cells) (Figure 5A-a, b; 22.8%−>6.8%) or anti-NK1.1 and TCRβ mAb (total NKT cells, including NKT-like cells) (Figure 5A-c, d; 27.9%−>6.6%). To detect the subset of type II NKT cells and NKT-like cells in the iNKT cell-deficient strains, the latter combination was employed. Although a significant decrease was demonstrated in NKT cells in WT mice (Figure 5B-a), there was no significant difference in the proportion of total NKT cells in Jα18$^{-/-}$ and CD1d$^{-/-}$ mice fed an HFD (Figure 5B-a), but Jα18$^{-/-}$ mice appeared to exhibit a slight decrease in the prevalence of these cells on an HFD. To examine the residual NKT-like cells in the livers of Jα18$^{-/-}$ and CD1d$^{-/-}$ mice, staining with a combination of anti-NK1.1 and anti-TCRβ mAb was employed. As demonstrated in the FACS profiles, total NKT cells in WT mice were significantly decreased after HFD feeding (Figure 5B-a). As for the subset of residual NKT cells, the subset that expressed neither CD4 nor CD8 (CD4$^-$8$^-$ double negative; DN) did not differ regardless of the feeding regimen used or the mouse strains analyzed. The relative prevalence of the CD4$^+$8$^-$ subset was as follows: WT>Jα18$^{-/-}$>CD1d$^{-/-}$ mice, and the prevalence of the CD4$^-$8$^+$ subset had an inverse relationship with CD8$^+$ cells (WT<Jα18$^{-/-}$<CD1d$^{-/-}$ mice) (Figure 5B-b, c). Although the total number of liver NKT cells was reduced, the residual population was mainly a CD4$^+$ subset in WT mice and the remaining cells were a CD4$^-$8$^-$ subset (Figure 5B-d). The CD8$^+$ subset was very minimal in WT mice. On the other hand, CD1d$^{-/-}$ mice had residual numbers of hepatic NK1.1$^+$TCRβ$^+$, NKT-like cells, and about 40~50% of the population was CD8$^+$. There was no significant difference in the proportion of regulatory T (T_{reg}) cells in HMNC among the three strains of mice (data not shown). It should be noted that NKT cells in the liver of WT mice fed with HFD were significantly reduced. This effect of lipid excess was evident as early as day 1 of HFD feeding (data not shown).

Analysis of infiltrated cellular components in adipose tissue of mice fed an HFD

The SVF in adipose tissue contains innate lymphocytes and Mϕ even under normal conditions. In adipose tissue in obese mice, we

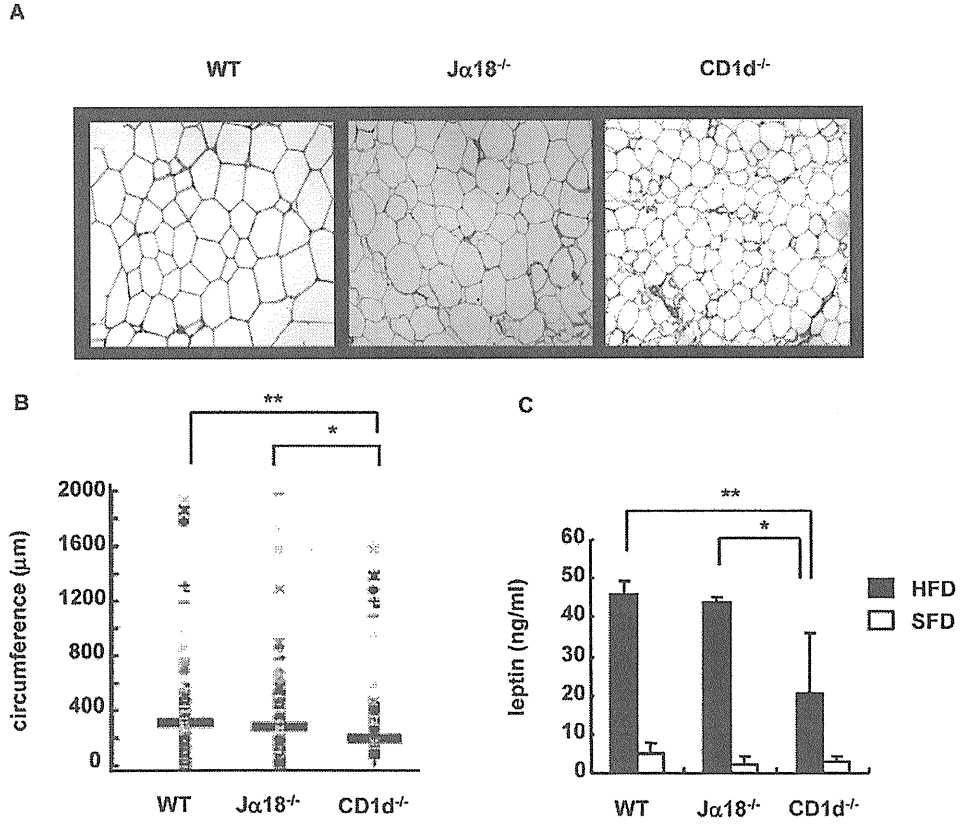

Figure 4. Histology of perigonadal adipose tissue and serum leptin level. (A, B) A paraffin section of perigonadal adipose tissue was stained with HE, and the circumference of adipocytes was morphometrically analyzed (10×10, 300–400 adipocytes measured) in HFD mice. (C) The serum leptin level was quantified by ELISA (n = 3–4 female mice in each group). Representative data of two similar experiments are shown. The results are expressed as mean ± s.d. Statistical analysis was performed according to the Tukey-Kramer test. *$p<0.05$, **$p<0.01$.
doi:10.1371/journal.pone.0030568.g004

readily detected increased numbers of mononuclear cells than in lean mice in spaces surrounded by adipocytes (data not shown). First, we analyzed NK1.1$^+$TCRβ$^+$ (NKT) cells and the CD4/8 subsets. Since the CD1d-restricted NKT cells are absent in CD1d$^{-/-}$ mice, we used NK1.1$^+$TCRβ$^+$ staining to detect residual NKT-like cells instead of double stainig with a combination of α-GalCer-loaded CD1d-dimers and anti-TCRβ mAb. In WT mice, the proportion of iNKT cells in adipose tissue was not significantly different (Figure 6A-a, b; 1.5%−>1.2%), whereas there were significantly more NK1.1$^+$TCRβ$^+$ cells in mice fed an HFD compared to those on SFD, in the same experimental setting (Figure 6A-c, d; 2.2%−>5.2%). The percentage of NKT cells increased in WT and Jα18$^{-/-}$ cells when the NKT cells of mice on HFD were compared with those on SFD (WT; $p<0.05$; Jα18$^{-/-}$; $p<0.01$), whereas such an increase was not observed in CD1d$^{-/-}$ mice (Figure 6B-a). Since CD1d$^{-/-}$ mice lack CD4$^+$ CD1d-restricted NKT cells, there were significant differences in the percentages (Figure 6B-b) (WT; $p<0.05$; Jα18$^{-/-}$; $p<0.01$) and actual cell numbers (WT, Jα18$^{-/-}$; $p<0.05$). Of note, the CD8$^+$ subset was prominently increased in the adipose tissue of Jα18$^{-/-}$ mice both in percentage (Figure 6B-c) and in number. The CD4$^-$8$^-$ subset of NKT cells appeared to be significantly decreased in Jα18$^{-/-}$ mice fed an HFD, most likely due to the relative abundance of the CD4$^-$8$^+$ subset (Figure 6B-d). Similar results were obtained when analyzing actual cell numbers (WT>Jα18$^{-/-}$>CD1d$^{-/-}$) (data not shown).

We analyzed and compared the proportion of NKT cells at early and late phases (18-wk) of HFD feeding. In WT mice, the number of α-GalCer-CD1d-dimer$^+$ cells and NK1.1$^+$TCRβ$^+$ cells in liver were increased at 1 wk of HFD-feeding, and numbers tended to decrease thereafter (Figure S3A). On the other hand, these cells, especially the NK1.1$^+$TCRβ$^+$ population, were gradually increased in adipose tissue (Figure S3B). The increase in NK1.1$^+$TCRβ$^+$ cells (percentage in SVF) in adipose tissue correlated with BW in WT and Jα18$^{-/-}$ mice, whereas no correlation was found in CD1d$^{-/-}$ mice (Figure 6C). A similar correlation was obtained between numbers of NK1.1$^+$TCRβ$^+$ cells (cell number/g adipose tissue) and BW (data not shown).

Analysis of Mφ in adipose tissue and cytokine production upon LPS stimulation

Mφ are another major cellular subset in SVF and may affect the metabolism of adipose tissue. Therefore, SVF preparations from the three strains of mouse were stained with F4/80 and CD11b (Figure 7A). The three strains had a similar pattern of F4/80$^+$/CD11b$^+$ staining. Although we anticipated that CD1d$^{-/-}$ mice had fewer Mφ than Jα18$^{-/-}$ mice, the percentage of F4/80$^+$/CD11b$^+$ cells in CD1d$^{-/-}$ mice was higher than that of Jα18$^{-/-}$ mice (Figure 7B-a). However, when the F4/80$^+$ population was divided into two subpopulations according to the MFI of F4/80 staining pattern, i. e., Population 1 (P1: F4/80^{high}) and Population 2 (P2: F4/80$^{low\sim-}$) cells (both CD11b$^+$), WT mice had higher frequencies of P1 than Jα18$^{-/-}$ mice (Figure 7B-b), whereas CD1d$^{-/-}$ mice had an increased frequency of P2 than WT and Jα18$^{-/-}$ mice (Figure 7B-c). Analyses of actual cell numbers

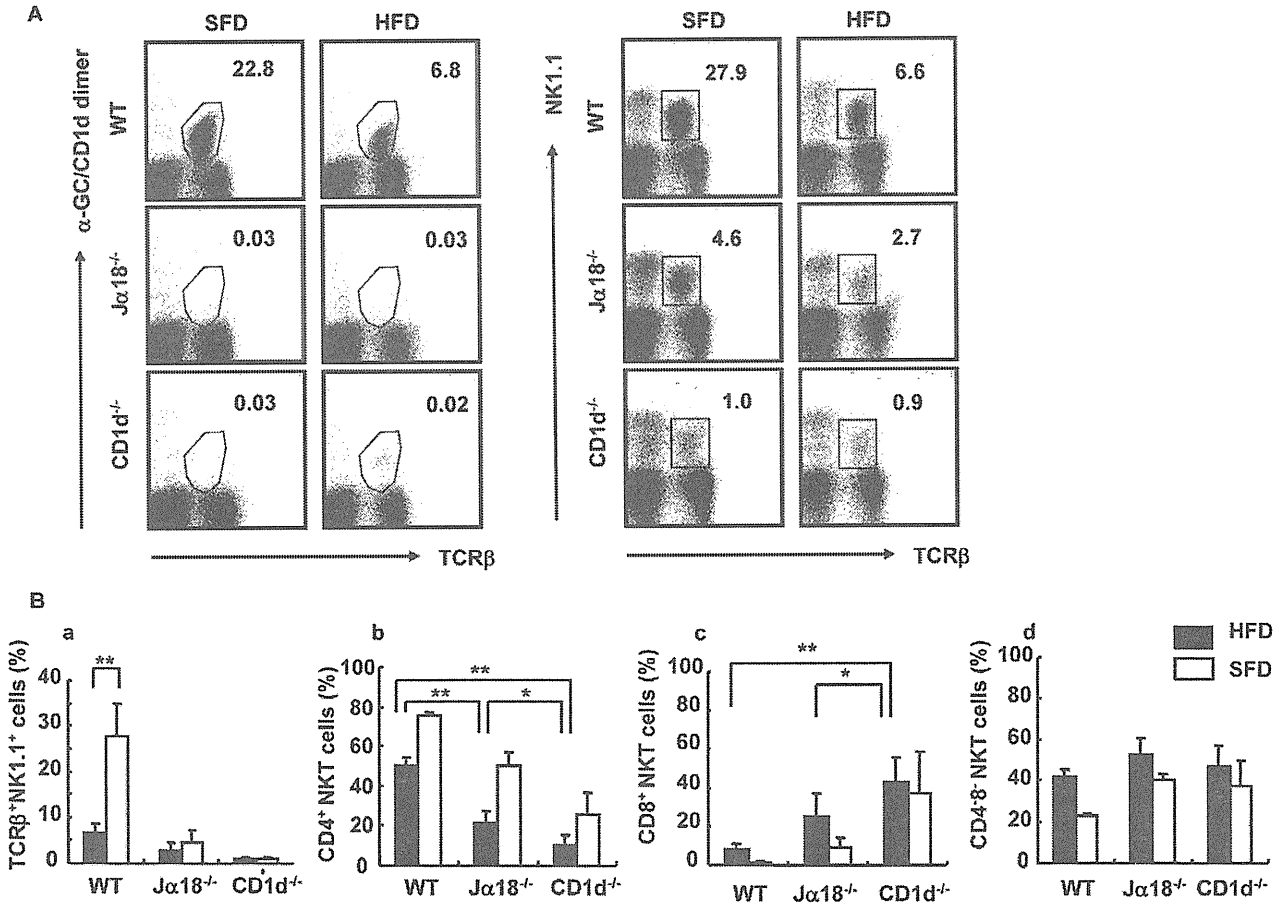

Figure 5. Flow cytometric analyses of HMNC in mice fed an SFD or an HFD. (A) A representative flow cytometric dot-plot defining the population of α-GalCer/CD1d dimer$^+$TCRβ$^+$ and NK1.1$^+$TCRβ$^+$ cells in the liver of SFD-fed mice (a, c) and HFD-fed mice (b, d). (B) The proportion of NK1.1$^+$TCRβ$^+$ cells (a), CD4$^+$ (b), CD8$^+$ (c), and CD4$^-$CD8$^-$ (d) NKT cells (n = 3–6 female mice in each group). Representative data of three similar experiments are shown. The results are expressed as mean ± s.d. Statistical analysis was performed according to the Tukey-Kramer test. *$p<0.05$, **$p<0.01$.

doi:10.1371/journal.pone.0030568.g005

demonstrated the same tendency among the three mouse strains (data not shown). Of note, a higher MFI of CD1d expression was detected in the cells of the P1 population compared with the P2 population, both in WT and Jα18$^{-/-}$ mice (Figure 7C-a, b, c).

To examine functional differences in a specific Mϕ population, total cells from the SVF fraction were stimulated with LPS for 20 h and cytokines were measured (Figure 8). IL-10 levels were significantly higher in SVF cultures from CD1d$^{-/-}$ mice compared with WT mice (Figure 8A), and GM-CSF was significantly lower in Jα18$^{-/-}$ and CD1d$^{-/-}$ mice (Figure 8B). Notably, the production of TNF-α in the culture supernatant that could affect insulin resistance was not significantly different among the three strains (Figure 8C).

Glucose and insulin tolerance are ameliorated CD1d$^{-/-}$ mice

Since the pattern of adiposity should reflect levels of glucose intolerance, IPGTT was performed in the three mouse strains (Figure 9). No difference was observed in fasting blood sugar levels and in elevation after *i.p.* administration of glucose over time in the three strains fed an SFD (Figure 9A, left). On the other hand, CD1d$^{-/-}$ mice demonstrated the lowest fasting blood sugar level and a suppressed elevation profile after glucose administration among the three strains on an HFD (Figure 9A, right). Insulin levels were significantly higher in WT and Jα18$^{-/-}$ mice before and at 120 min after infusion than that obtained in the respective groups on an SFD (data not shown) and for CD1d$^{-/-}$ mice on an HFD, suggesting that insulin resistance was present in those strains (Figure 9B). To further examine insulin resistance, an ITT was performed in HFD-fed mice that had been fasted for 3.5 h [6] (Figure 9C). Following injection of insulin, blood glucose levels fell most prominently in CD1d$^{-/-}$ mice at 30 and 60 min after the injection (Figure 9C). The decrease in glucose level in WT mice injected with α-GalCer was less than that of mice injected with vehicle (Figure S1B), suggesting that insulin resistance was reproduced in mice when iNKT cells were activated [18], although there was no net increase in BW with the treatment. Thus, CD1d$^{-/-}$ mice developed the least resistance to insulin in the absence of both iNKT and type II NKT cells.

To examine whether type II NKT cells alone could reproduce the pathophysiological status observed in Jα18$^{-/-}$ mice, HMNC obtained from either Jα18$^{-/-}$ or CD1d$^{-/-}$ mice were intravenously transferred to CD1d$^{-/-}$ recipient mice and weight gain was examined on an HFD. CD1d$^{-/-}$ mice that received HMNC from Jα18$^{-/-}$ mice showed a slight increase in BW and exhibited a less profound decrease in blood glucose levels in the ITT (Figure S4A, C). Although no significant difference was detected with the IPGTT (Figure S4B), CD1d$^{-/-}$ mice that received HMNC from